Supporting Information

A new superacid hafnium-based metal-organic framework as a highly active heterogeneous catalyst for the synthesis of benzoxazoles under solvent-free condition

Linh H. T. Nguyen,[a] The T. Nguyen,[b] Ha L. Nguyen,[a] Tan L. H. Doan,*[,a,b] Phuong Hoang Tran*[,b]

[a]Center for Innovative Materials and Architectures (INOMAR), Vietnam National University – Ho Chi Minh City (VNU-HCM), Ho Chi Minh City 721337, Vietnam

[b]Faculty of Chemistry, University of Science, VNU-HCM, Ho Chi Minh City 721337, Vietnam

*To whom correspondence should be addressed: dlhtan@inomar.edu.vn,

thphuong@hcmus.edu.vn

Table of Contents

Section S1: Materials and General Methods

Materials.

Methyl 4-iodobenzoate (purity > 97%), 1,4-diethynylbenzene (purity > 96%), copper(I) iodide (purity ≥ 99.5%), 1,3,5-Benzenetricarboxylic acid (H_3BTC, purity > 95%), 1,4-benzenedicarboxylic acid (H_2BDC, purity > 98%), hafnium chloride ($HfCl_4$, purity >98%), sulfuric acid (H_2SO_4, purity ≥ 95%), hydrofluoric acid (HF, 48 wt% in water), anhydrous benzene (C_6H_6, purity > 99%), anhydrous chloroform a with amylenes as stabilizer ($CHCl_3$, purity > 99%), (-)-isopulegol ($C_{10}H_{18}O$, purity > 99%), camphene ($C_{10}H_{16}$, analytical standard), (R)-(+)-limonene ($C_{10}H_{16}$, analytical standard), benzaldehyde (purity ≥ 99%), 4-methylbenzaldehyde (purity ≥ 97%), 4-methoxybenzaldehyde (purity ≥ 98%), 4-*tert*-butylbenzaldehyde (purity ≥ 97%), 4-fluorobenzaldehyde (purity ≥ 98%), 4-chlorobenzaldehyde (purity ≥ 97%), 4-bromobenzaldehyde (purity ≥ 99%), 4-hydroxybenzaldehyde (purity ≥ 98%), anhydrous aluminum chloride ($AlCl_3$, purity ≥ 99%), anhydrous iron(III) chloride ($FeCl_3$, purity ≥ 97%), anhydrous copper(II) acetate ($Cu(CH_3COO)_2$, purity ≥ 98%), anhydrous zinc chloride ($ZnCl_2$, purity ≥ ≥97%), HKUST-1 (Basolite C300), MOF-177 (Basolite Z377), and ZIF-8 (Basolite Z1200), and sigmacote® siliconizing reagent for glass and other surfaces were obtained from Sigma-Aldrich Chemical Company.

Zirconium oxychloride octahydrate ($ZrOCl_2 \cdot 8H_2O$, purity ≥ 99.5%), hafnium oxychloride octahydrate ($HfOCl_2 \cdot 8H_2O$, purity ≥ 99.5%) were obtained from Alfa Aesar.

N,N-Dimethylformamide (DMF, purity > 99%), ammonium chloride (NH_4Cl, purity 99.5%, bis(triphenylphosphine)palladium dichloride (purity ≥ 99%), potassium hydroxide (purity > 99%), sodium chloride (NaCl, purity ≥ 99%), 2-aminophenol (purity ≥ 99%), 2-amino-4-methylphenol (purity ≥ 97%), 2-amino-4-chlorophenol (purity ≥ 97%), and 2-amino-4-nitrophenol (purity ≥ 99%) were obtained from Acros Organics.

Formic acid (HCOOH, purity > 98%), triethylamine (TEA, purity ≥ 99.5%), methanol (MeOH, purity ≥ 99.8%), and silica gel 230–400 mesh for flash chromatography, TLC plates (silica gel 60 F254), anhydrous 1,4-dioxane (purity ≥ 99.9%), anhydrous ethanol (EtOH, purity ≥ 99%), anhydrous toluene (purity ≥ 99%), anhydrous dichloromethane (CH_2Cl_2, 99%), anhydrous *n*-butanol (purity ≥ 99.8%), anhydrous tetrahydrofuran (THF, purity ≥ 99.5%), anhydrous ethyl acetate (EtOAc, purity ≥ 99%), acetone, and *n*-hexane (purity ≥ 99.5%) were obtained from Merck.

Deuterated solvents, $CDCl_3$, acetone-d_6 and DMSO-d_6, were purchased from Cambridge Isotope Laboratories (Andover, MA).

Hammett Indicators: 4-Phenylazoaniline (analytical standard), 4-nitrodiphenylamine (purity ≥ 99%), 9,10-anthraquinone (purity ≥ 97%), 4-fluoronitrobenzene (purity ≥ 99%), 2,4-dichloro-6-nitroaniline (purity > 98%), 2-benzoylnaphthalene (purity ≥ 98%), and 2-bromo-4,6-dinitroaniline (purity ≥ 98.0%) were obtained from Sigma-Aldrich Co. 2,4-dinitrofluorobenzene (purity 98%) was obtained from Acros Co. All chemicals were used without further purification.

General Methods.

Single-crystal X-ray diffraction (SXRD) data were collected using synchrotron radiation in beamline 11.3.1 of the Advanced Light Source, Lawrence Berkeley National Laboratory (LBNL). Powder X-ray diffraction (PXRD) patterns were recorded using a D8 Advance diffractometer equipped with a LYNXEYE detector (Bragg-Brentano geometry, Cu Kα radiation λ = 1.54056 Å. Fourier transform infrared (FT-IR) spectra were measured on a Bruker E400 FT-IR spectrometer using potassium bromide pellets. Scanning electron microscope (SEM) images were obtained using a Hitachi's S-4800 FE-SEM. Transmission Electron Microscopy (TEM) images were performed on a JEOL JEM-2100F. Low-pressure N_2 and CO_2 adsorption measurements were carried out on a Quantachrome Autosorb iQ volumetric gas adsorption analyzer. A liquid N_2 bath was used for measurements at 77 K. Helium was used as estimation of dead space. Ultrahigh-purity-grade N_2, and He (99.999% purity) were used throughout adsorption experiments. Solution NMR spectra were acquired on a Bruker Advance-500 MHz NMR spectrometer. For NMR measurements of MOF, 10 mg of MOF sample was digested in a mixture containing 580 μL of DMSO-d_6 and 20 μL of hydrofluoric acid (48 wt% in water) and sonicated for 15 min. Carbon, hydrogen, nitrogen and sulfur elemental microanalyses (EA) were performed in the Microanalytical Laboratory of the College of Chemistry at UC Berkeley, using a Perkin Elmer 2400 Series II CHNS elemental analyzer. ICP-MS analyses were performed on a PerkinElmer NexION 350X.

Section S2: Synthesis and Preparation of MOFs

HKUST-1 (Basolite C300), MOF-177 (Basolite Z377), and ZIF-8 (Basolite Z1200) were obtained from Sigma-Aldrich Chemical Co. Before HKUST-1, MOF-177, and ZIF-8 were used as heterogeneous catalysts in the reaction, the materials were activated under vacuum (30 mTorr) for 24 h at 120, 150, 100 °C, respectively.

Microcrystalline powder sample of VNU-11-P. A mixture of H_3BTC (2.50 mmol, 537 mg) and $HfOCl_2 \cdot 8H_2O$ (7.50 mmol, 3.10 g) were dissolved in DMF/formic acid (160 mL/160 mL) and placed in a 500 mL screw-capped glass jar, which was heated to 120 °C for three days. A white precipitate was collected by filtration and washed three times with 100 mL of fresh DMF and immersed in 100 ml DMF for three days, during which time the DMF was replaced three times per day. The DMF-exchanged compound was filtrated off and immersed in 100 mL of water for three days, during which time the water was replaced three times per day. Water exchanged material was then immersed in 100 mL of anhydrous acetone for three days, during which time the acetone was replaced three times per day. The acetone-exchanged sample was then evacuated at room temperature for 24 h and at 150 °C for 24 h to yield activated sample (Yield: 2.30 g, 74 % based on $HfOCl_2 \cdot 8H_2O$). Digested ^{1}H-NMR of activated sample (500 MHz, DMSO-d_6, ppm): 8.64 (s, BTC), 8.12 (s, HCOOH), peak area ratio (BTC:HCOOH) = 6.0:5.0. Anal. Calcd for $Hf_6C_{23}H_{14}O_{30}$ = $[Hf_6O_5(OH)_3(C_9H_3O_6)_2(HCOO)_5]$: Hf, C, 15.00; H, 0.76%. Found: C, 14.95; H, 0.89%.

Single crystal sample of VNU-11-SC. A mixture of H_3BTC (0.0125 mmol, 2.62 mg) and $HfOCl_2 \cdot 8H_2O$ (0.0125 mmol, 5.11 mg) were dissolved in DMF/formic acid (6.4 mL/6.4 mL) and placed in a 20 mL screw-capped glass jar, which was heated to 110 °C for seven days. Octahedral colorless crystals were collected and washed three times with 10 mL of fresh DMF. Digested ^{1}H-NMR of as-synthesized sample (500 MHz, DMSO-d_6, ppm): 8.64 (s, BTC), 8.12 (s, HCOOH), peak area ratio (BTC:HCOOH) = 6.0:5.0. Anal. Calcd for $Hf_6C_{23}H_{14}O_{30}$ = $[Hf_6O_5(OH)_3(C_9H_3O_6)_2(HCOO)_5]$: C, 15.00; H, 0.76%. Found: C, 15.07; H, 0.83%.

Microcrystalline powder sample of VNU-11-P-SO_4. Activated VNU-11-P microcrystalline powder (200 mg, 0.109 mmol) was immersed in 20 mL of 0.1 M sulfuric acid (2.00 mmol) for 24 h during which time the mixture was stirred about once every two hours. The solid material was thoroughly washed with deionized water (3 x 20 ml per day for three days total), quickly

exchanged with 5 x 20 ml anhydrous acetone. To obtain guest-free material, VNU-11-P-2.5SO_4 was immersed in anhydrous chloroform (3 x 20 ml per day over a total of three days). The solvent exchanged sample was activated under vacuum for 24 h at room temperature and 24 h at 150 ^oC to get activated VNU-11-P-2.5SO_4 (Yield 195 mg). Digested ^{1}H-NMR of activated sample (500 MHz, DMSO-d_6, ppm): 8.64 (s, BTC), 8.12 (s, HCOOH), peak area ratio (BTC:HCOOH) = 6.0:0.06. Anal. Calcd for $Hf_6C_{18.06}H_{11}O_{31.06}S_{2.5}$ = $[Hf_6O_5(OH)_{2.94}(C_9H_3O_6)_2(SO_4)_{2.5}(HCOO)_{0.06}](H_2O)$: C, 11.56; H, 0.59; S, 4.27%. Found: C, 11.89; H, 0.68; S, 4.05%.

Single crystal sample of VNU-11-SC-SO_4: Octahedral colorless crystals VNU-11 were collected and washed three times with 10 mL of fresh DMF and immersed in deionized water (3 x 20 ml per day for three days total). Roughly 50.0 mg VNU-11-SC was immersed in 5 mL of 0.1 M sulfuric acid (2.00 mmol) for 24 h during which time the mixture was stirred about once every two hours. The single crystals was thoroughly washed with deionized water (3 x 20 ml per day for three days total), quickly exchanged with 5 x 20 ml anhydrous acetone. To obtain guest-free material, VNU-11-SC-2.3SO_4 was immersed in anhydrous chloroform (3 x 20 ml per day over a total of 3 days). The solvent exchanged crystals was activated under vacuum for 24 h at room temperature and 24 h at 150 ^oC to get activated VNU-11-SC-2.3SO_4 (Yield 48.5 mg). Digested ^{1}H-NMR of activated sample (500 MHz, DMSO-d_6, ppm): 8.64 (s, BTC), 8.12 (s, HCOOH), peak area ratio (BTC:HCOOH) = 6.0:0.08. Anal. Calcd for $Hf_6C_{18.08}H_{24.6}O_{37.28}S_{2.3}$ = $[Hf_6O_{5.4}(OH)_{2.52}(C_9H_3O_6)_2(SO_4)_{2.3}(HCOO)_{0.08}](H_2O)_8$: C, 10.95; H, 1.25; S, 3.72%. Found: C, 11.20; H, 1.18; S, 4.04%.

Microcrystalline powder sample of MOF-808-P: Synthesis of MOF-808-P was slightly modified from reported literature.[1] A mixture of H_3BTC (2.50 mmol, 537 mg) and $ZrOCl_2 \cdot 8H_2O$ (7.50 mmol, 2.42 g) were dissolved in DMF/formic acid (160 mL/160 mL) and placed in a 500 ml screw-capped glass jar, which was heated to 120 °C for three days. A white precipitate was collected by filtration and washed three times with 100 mL of fresh DMF and immersed in 100 ml DMF for three days, during which time the DMF was replaced three times per day. The DMF-exchanged compound was filtrated off and immersed in 100 mL of water for three days, during which time the water was replaced three times per day. Water exchanged material was then immersed in 100 mL of anhydrous acetone for three days, during which time the acetone

was replaced three times per day. The acetone-exchanged sample was then evacuated at room temperature for 24 h and at 150 °C for 24 h to yield activated sample.

Microcrysalline powder MOF-808-P-2.5SO_4: Synthesis of MOF-808-P-2.5SO_4 was slightly modified from reported literature.[1] Activated MOF-808-P microcrystalline powder (200 mg, 0.151 mmol) was immersed in 20 mL of 0.1 M sulfuric acid (2.00 mmol) for 24 h during which time the mixture was stirred about once every two hours. The solid material was thoroughly washed with deionized water (3 x 20 ml per day for three days total), quickly exchanged with 5 x 20 ml anhydrous acetone. To obtain guest-free material, MOF-808-P-2.5SO_4 was immersed in anhydrous chloroform (3 x 20 ml per day over a total of 3 days). The solvent exchanged sample was activated under vacuum for 24 h at room temperature and 24 h at 150 ^oC to get MOF-808-P-2.5SO_4 (Yield 195 mg).

Microcrystalline powder sample of UiO-66. Synthesis of UiO-66 was modified from reported literature.[2] $ZrOCl_2 \cdot 8H_2O$ (109 mg, 0.340 mmol) and 1,4-benzene-dicarboxylic acid (56.5 mg, 0.340 mmol) in 40 mL solvent mixture of DMF and acetic acid (v/v = 39:1) in 100-mL capped bottle was heated in an oven at 120 °C for 24 h under static conditions. After cooling the vial to room temperature, the white precipitate product, UiO-66, was separated from the mother liquor via centrifugation. The as-synthesized sample of UiO-66 was washed with 10 mL of DMF three times per day over the course of three days. Then UiO-66 was immersed in 10 mL chloroform, which was replaced three times per day for a total of three days. After the solvent-exchange process was completed, UiO-66 was activated under reduced pressure at 120 °C for 24 h.

Preparation of 1,4-bis(2-[4-carboxyphenyl]ethynyl)benzene (H_2CPEB). 1,4-Bis(2-[4-carboxyphenyl]ethynyl)benzene was prepared following a literature procedure.[3] The Sonogashira coupling of methyl 4-iodobenzoate (0.524 g, 2.00 mmol) and 1,4-diethynylbenzene (0.126 g, 1.00 mmol) was catalyzed by bis(triphenylphosphine)palladium dichloride (35.2 mg, 0.0500 mmol) and copper(I) iodide (2.0 mg, 10 μmol) in 10 mL mixture of triethylamine and toluene (v/v = 1:1) under nitrogen atmosphere. The solution was stirred at room temperature for 24 h. After the reaction, the solid was filtered, thoroughly washed with hexane, a saturated solution of NH_4Cl, and a saturated solution of NaCl, and dried under vacuum to afford pink product. Then the precursor (0.985 g, 0.250 mmol) was hydrolyzed by potassium hydroxide (0.420 g, 7.50 mmol) in mixture of methanol (3 mL), THF (3 mL) and water (1.5 mL) at room temperature for

12 h. After 12 h, the solvents were evaporated under reduced pressure and the remaining solution was added dropwise of concentrated HCl. The final product was recovered as a yellow powder, which was thoroughly washed with water and dried at 80 °C under vacuum overnight. Yield: 0.0780 g.

Microcrystalline powder sample of VNU-1. VNU-1 microcrystalline powder sample was prepared following the reported procedure[3] $ZrOCl_2 \cdot 8H_2O$ (10.9 mg, 0.0340 mmol) and H_2CPEB (12.4 mg, 0.0340 mmol) were dissolved in a solvent mixture of DMF (3.86 mL), acetic acid (0.042 mL), and water (0.10 mL) in a 10 mL capped vial. The solution was subsequently heated at 120 °C for 1 day in an isothermal oven to yield yellow precipitate. After cooling the vial to room temperature, the yellow precipitate product, VNU-1, was separated from the mother liquor via centrifugation. The as-synthesized sample of VNU-1 was washed with 10 mL of DMF three times per day over the course of three days. Following this, VNU-1 was immersed in 10 mL chloroform, which was replaced three times per day for a total of three days. After the solvent-exchange process was completed, VNU-1 was activated under reduced pressure at 120 °C for 24 h.

Microcrystalline powder sample of VNU-2. VNU-2 microcrystalline powder sample was prepared following the reported procedure.[3] $HfCl_4$ (10.9 mg, 0.0340 mmol) and H_2CPEB (12.4 mg, 0.0340 mmol) were dissolved in a solvent mixture of DMF (3.80 mL), acetic acid (0.10 mL), and water (0.10 mL) in a 10 mL capped vial. The solution was subsequently heated at 120 °C for 3 days in an isothermal oven to yield light yellow microcrystalline powder. After cooling the vial to room temperature, the light yellow solid product, VNU-2, was separated from the mother liquor via centrifugation. The as-synthesized sample of VNU-2 was washed with 10 mL of DMF three times per day over the course of three days. Following this, VNU-2 was immersed in 10 mL chloroform, which was replaced three times per day for a total of three days. After the solvent-exchange process was completed, VNU-2 was activated under reduced pressure at 120 °C for 24 h.

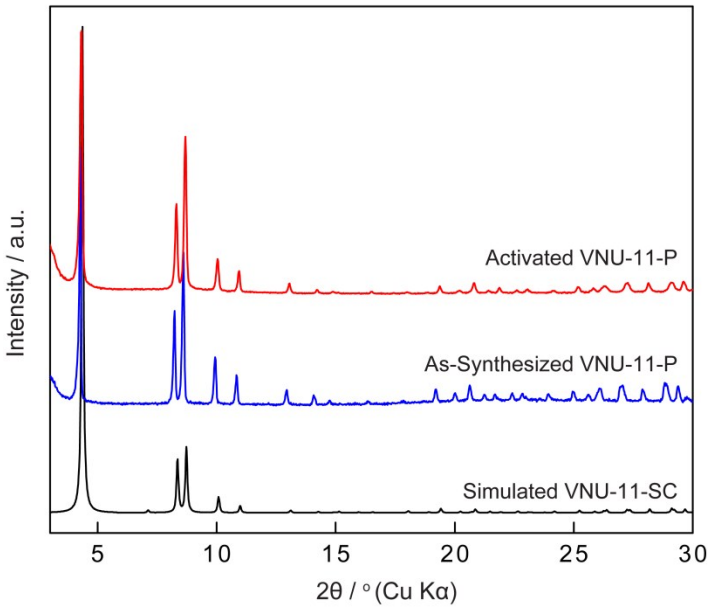

Fig. S1. PXRD analysis of VNU-11-P. The calculated pattern from single crystal data (black) is compared to the experimental patterns from the as-synthesized powder sample (blue) and activated powder sample (red).

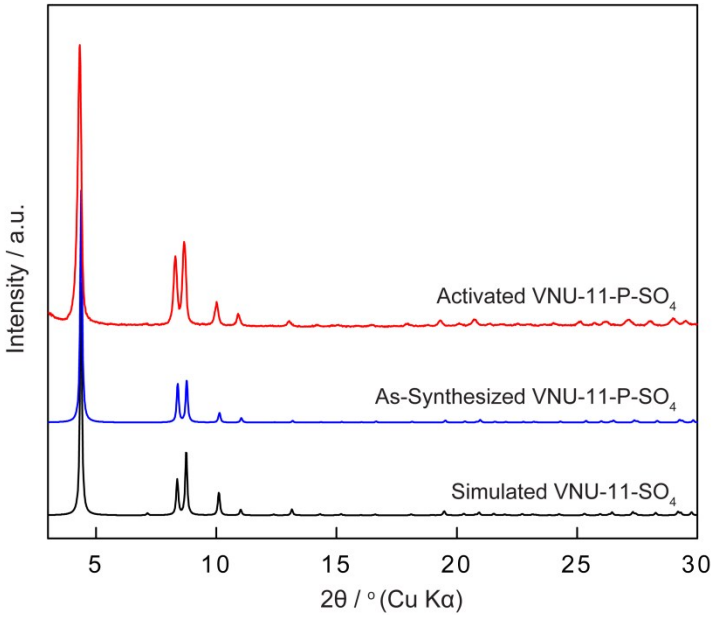

Fig. S2. PXRD analysis of VNU-11-P-SO_4. The calculated pattern from single crystal data (black) is compared to the experimental patterns from the as-synthesized powder sample (blue) and activated powder sample (red).

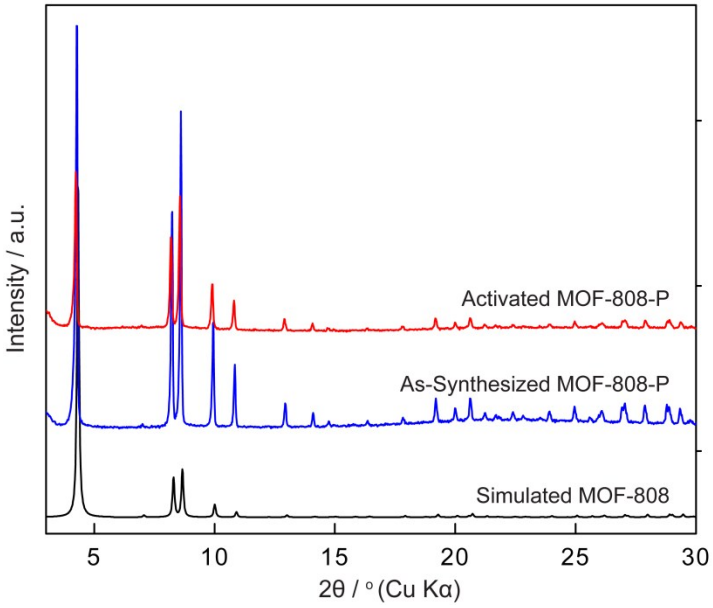

Fig. S3. PXRD analysis of MOF-808-P. The calculated pattern from single crystal data (black) is compared to the experimental patterns from the as-synthesized powder sample (blue) and activated powder sample (red).

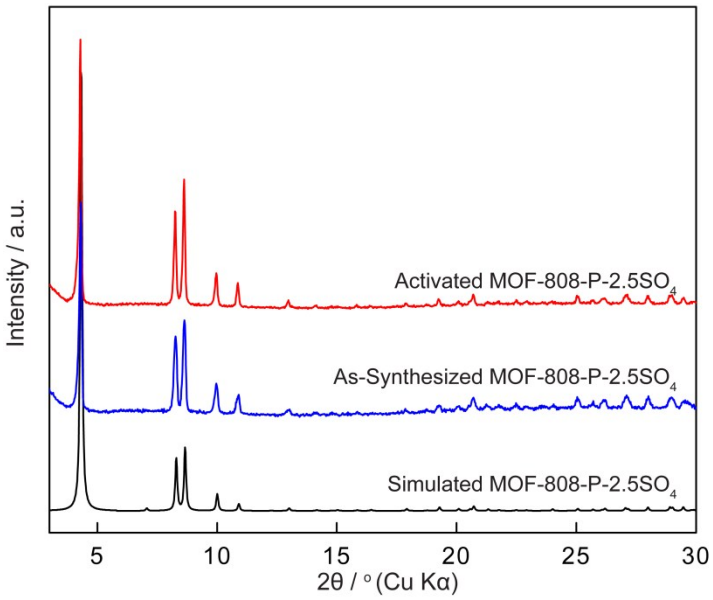

Fig. S4. PXRD analysis of MOF-808-P-2.5SO_4. The calculated pattern from single crystal data (black) is compared to the experimental patterns from the as-synthesized powder sample (blue) and activated powder sample (red).

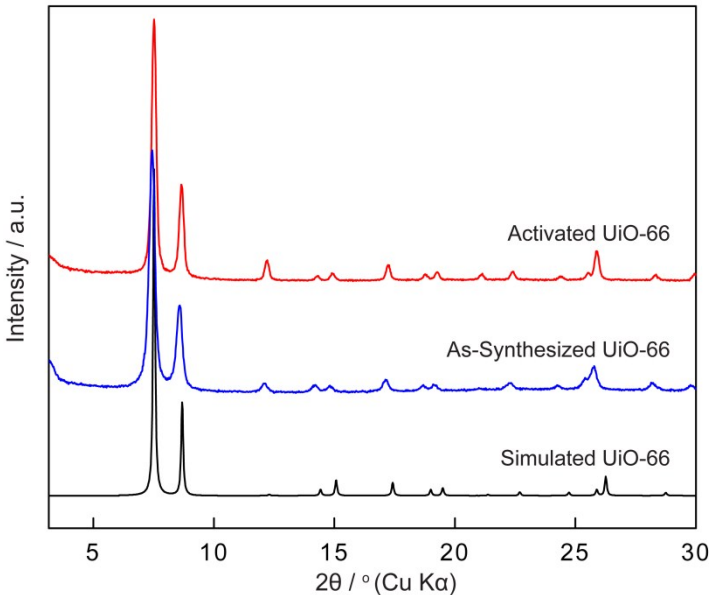

Fig. S5. PXRD analysis of UiO-66. The calculated pattern from single crystal data (black) is compared to the experimental patterns from the as-synthesized powder sample (blue) and activated powder sample (red).

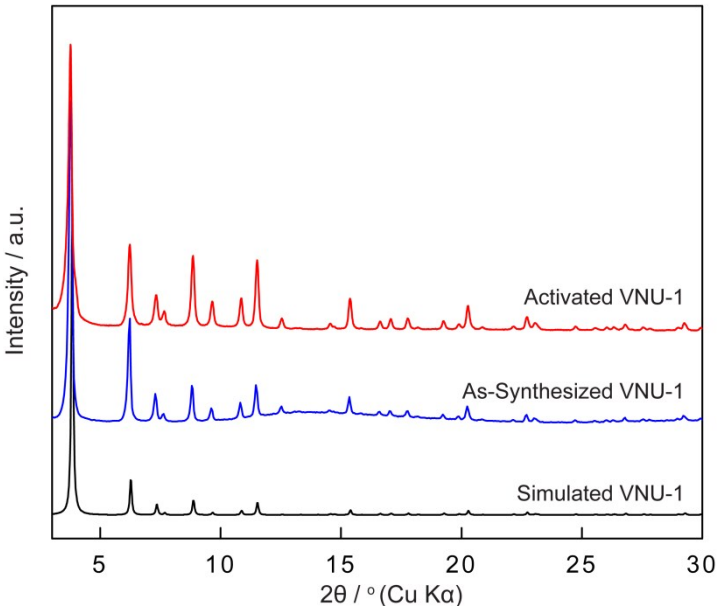

Fig. S6. PXRD analysis of VNU-1. The calculated pattern from single crystal data (black) is compared to the experimental patterns from the as-synthesized powder sample (blue) and activated powder sample (red).

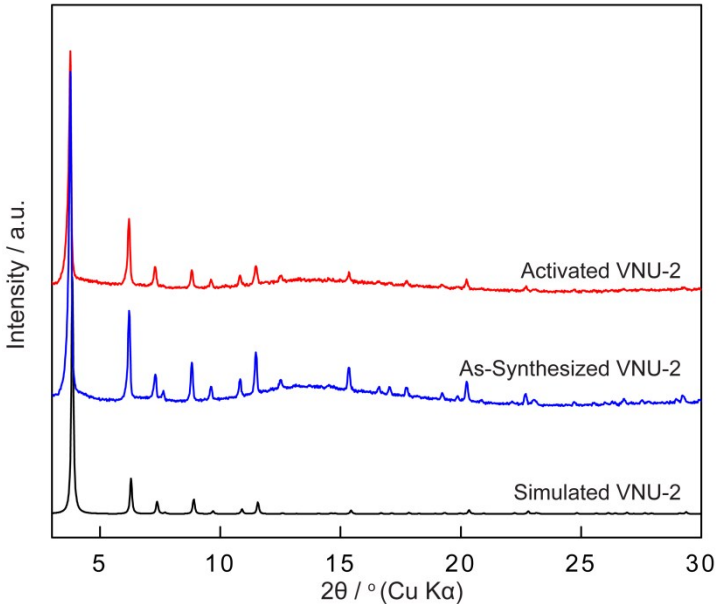

Fig. S7. PXRD analysis of VNU-2. The calculated pattern from single crystal data (black) is compared to the experimental patterns from the as-synthesized powder sample (blue) and activated powder sample (red).

Section S3: Single Crystal X-ray Diffraction Analyses

The X-ray diffraction data for VNU-11 and VNU-11-SO_4 was collected on a Bruker D8 Venture diffractometer outfitted with a PHOTON-100 CMOS detector using monochromatic microfocus MoKα radiation (λ = 0.71073 Å) that was operated at 50 kV and 1.0 mA. The data was collected at 100 K by chilled nitrogen flow controlled by a Kryoflex II system. Unit cell determination was performed in the Bruker SMART APEX II software suite. The data sets were reduced and a multi-scan spherical absorption correction was implemented in the SCALE interface. The structures were solved with direct methods and refined by the full-matrix least-squares method in the SHELXL-97 program package. Once the framework atoms were located in the difference Fourier maps, the SQUEEZE routine in PLATON was performed to remove scattering from disordered guest molecules residing in the pores. The detail of single crystal refinement for VNU-11 and VNU-11-SO_4 was found in Table S1 and Table S2. VNU-11 and VNU-11-SO_4 contain more void space, high electron density atoms, and high vibration atoms (SO_4^{2-}), leading to obtain low resolution to fully refinement. These factors cause few level A and B alerts in the check cif files, which are fully explained in the CIF file. CCDC numbers for VNU-11 and VNU-11-SO4 are 1560539 and 1560540, respectively.

Table S1. Crystal structure data and refinement of VNU-11 single crystal

Empirical formula	$C_{12}H_6O_{16}Hf_3$	
Formula weight	941.64	
Temperature	100 (2) K	
Wavelength	0.71073 Å	
Crystal system	Cubic	
Space group	*Fd*-3*m*	
Unit cell dimensions	$a = b = c$ = 34.9801(12) Å	$\alpha = 90°$ $\beta = 90°$ $\gamma = 90°$

Volume	42802(4) $Å^3$	
Z	32	
Density (calculated)	1.169 g cm^{-3}	
Absorption coefficient	5.836 mm^{-1}	
$F(000)$	13504	
Crystal size	0.1 × 0.1 × 0.09 mm^3	
Theta range for data collection	1.647 to 27.917°	
Index ranges	$0 \leq h \leq 46$, $0 \leq k \leq 46$, $0 \leq l \leq 46$	
Independent reflections	2453 [$R_{int} = 0.0663$]	
Completeness to theta = 27.917°	100%	
Absorption correction	Multi-scan	
Refinement method	Full-matrix least-squares on F^2	
Data / restraints / parameters	2453 / 0 / 57	
Goodness-of-fit on F^2	1.119	
Final R indices [$I > 2\sigma(I)$]	$R_1 = 0.0467$, $wR_2 = 0.1180$	
R indices (all data)	$R_1 = 0.0384$, $wR_2 = 0.1230$	
Largest diff. peak and hole	1.136 and -1.346 e·$Å^{-3}$	

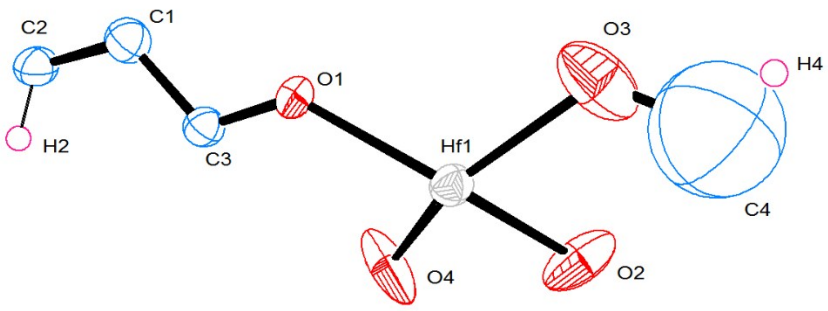

Fig. S8. Fragment unit of VNU-11 drawn by ORTEP with thermal ellipsoids style at 50% probability.

Table S2. Crystal structure data and refinement of VNU-11-SO_4 single crystal

Empirical formula	$C_9H_3O_{13}Hf_3S_{1.2}$	
Formula weight	893.06	
Temperature	100 (2) K	
Wavelength	0.71073 Å	
Crystal system	Cubic	
Space group	*Fd*-3*m*	
Unit cell dimensions	$a = b = c = 34.901(3)$ Å	$\alpha = 90°$ $\beta = 90°$ $\gamma = 90°$
Volume	42512(3) $Å^3$	
Z	32	
Density (calculated)	1.309 g cm^{-3}	
Absorption coefficient	5.931 mm^{-1}	
F(000)	15136	
Crystal size	0.1 × 0.1 × 0.09 mm^3	
Theta range for data collection	1.935 to 25.739°	
Index ranges	$0 \le h \le 42$, $0 \le k \le 42$, $0 \le l \le 42$	
Independent reflections	1962 [$R_{int} = 0.0544$]	

Completeness to theta = 25.739°	99%	
Absorption correction	Multi-scan	
Refinement method	Full-matrix least-squares on F^2	
Data / restraints / parameters	1962 / 1 / 64	
Goodness-of-fit on F^2	1.383	
Final R indices [$I > 2\sigma(I)$]	$R_1 = 0.062$, $wR_2 = 0.1518$	
R indices (all data)	$R_1 = 0.0491$, $wR_2 = 0.1461$	
Largest diff. peak and hole	2.007 and -1.498 e·Å^{-3}	

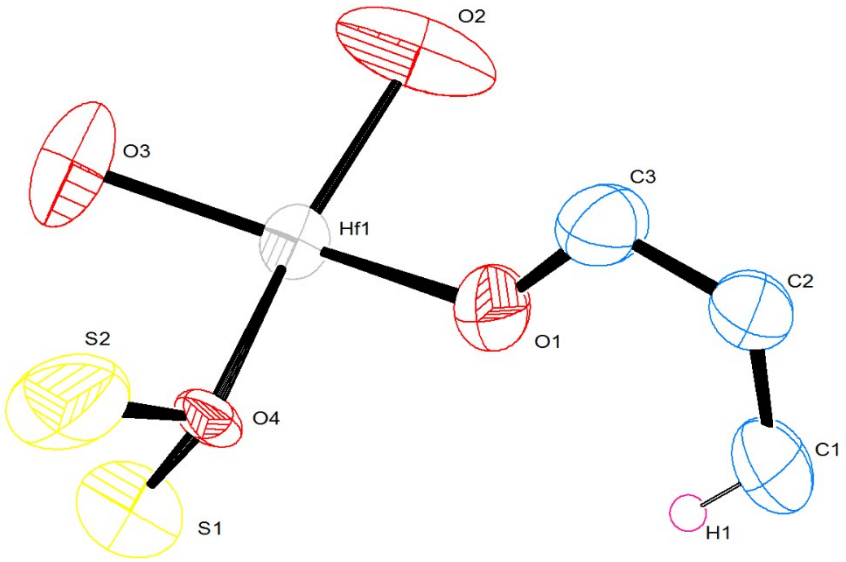

Fig. S9. Fragment unit of VNU-11-SO_4 drawn by ORTEP with thermal ellipsoids style at 50% probability.

Section S4: N_2 Adsorption Measurements

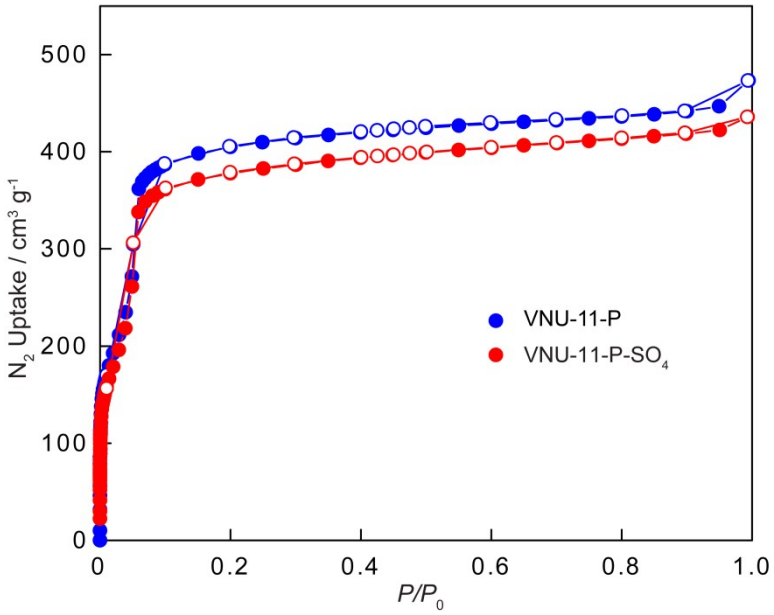

Fig. S10. N_2 isotherm at 77 K for activated VNU-11-P (blue) and VNU-11-P-SO_4 (red). Closed and open circles represent the adsorption and desorption branches, respectively.

Section S5: Infrared Spectra

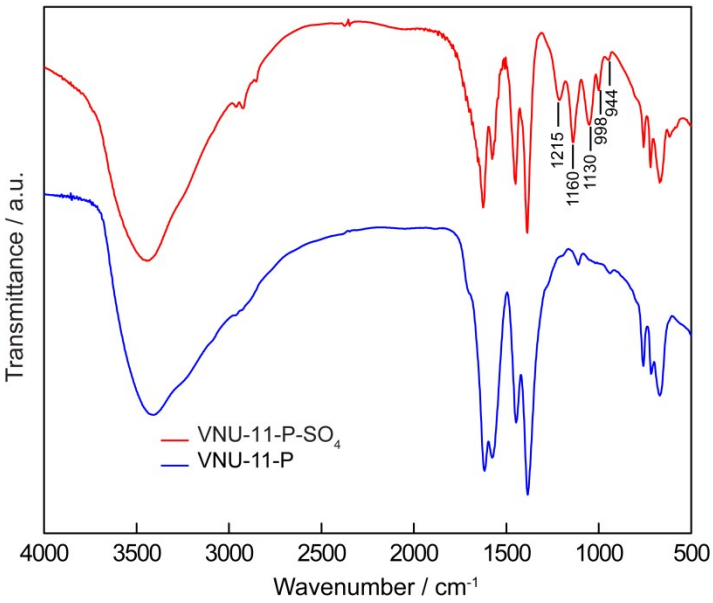

Fig. S11. Infrared spectra of activated VNU-11-P (blue) and VNU-11-P-SO_4 (red) in dry KBr.

Section S6: Hammett Indicator Tests

Hammett Indicators solutions was prepared following the reported procedure.[1] In an inert atmosphere, 5.0 mg of activated VNU-11-P-SO_4 was added in Hammett indicators solutions (Table S3), which were prepared by dissolving 1.0 mmol of indicators in 5 mL anhydrous benzene. The mixture was shaken for each 30 min, after 4 hours the color of the solid was then recorded (Table S3)

Table S3. Hammett Indicator tests of VNU-11-P-SO_4.

Indicators	Color		pK_a	Hammett Indicator Tests	
	Acid Form	Base Form		VNU-11-P	VNU-11-P -SO_4
4-Phenylazoaniline	Red	Orange	+2.8	-	+
4-Nitrodiphenylamine	Red	Yellow	-2.4	-	+
2,4-Dichloro-6-nitroaniline	Red	Yellow	-3.2	-	+
2-Benzoylnaphthalene	Yellow	Colorless	-5.9	-	+
2-Bromo-4,6-dinitroaniline	Red	Yellow	-6.6	-	+
Anthraquinone	Yellow	Colorless	-8.1	-	+
4-Fluoronitrobenzene	Yellow	Colorless	-12.4	-	+
2,4-Dinitrofluorobenzene	Yellow	Colorless	-14.5	-	+

Results of Hammett indicator tests are denoted as color change observed (+) and color change not observed (-).

Section S7: Scanning Electron Microscopy and Energy-Dispersive X-ray Spectroscopy

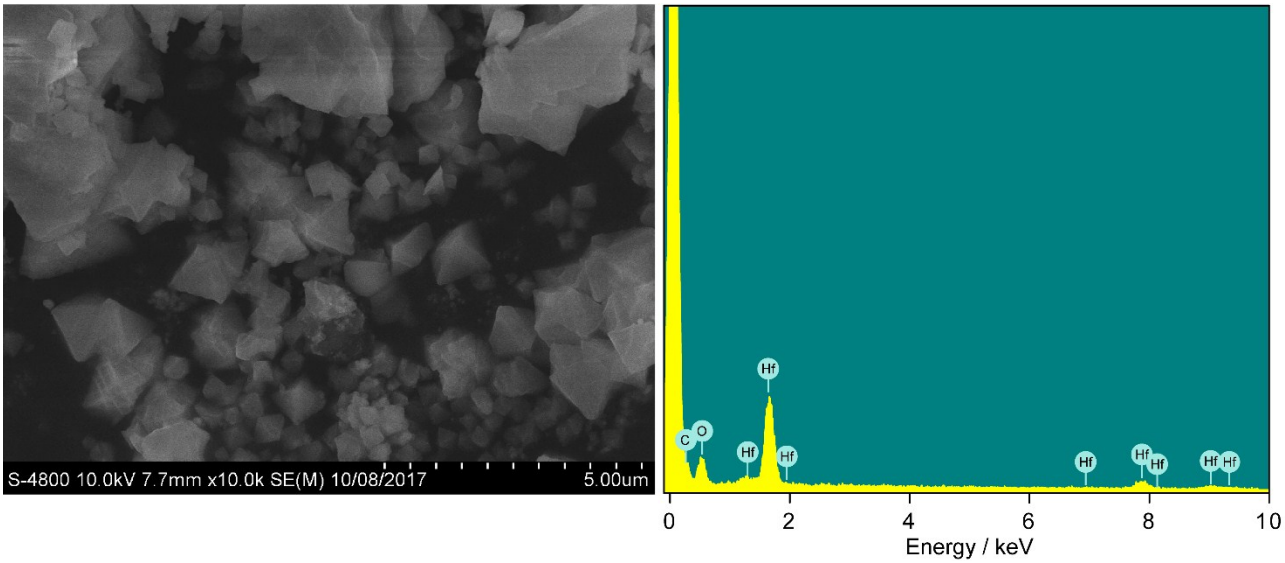

Fig. S12. Scanning electron microscopy (SEM) image and Energy-dispersive X-ray (EDX) spectrum of VNU-11-P.

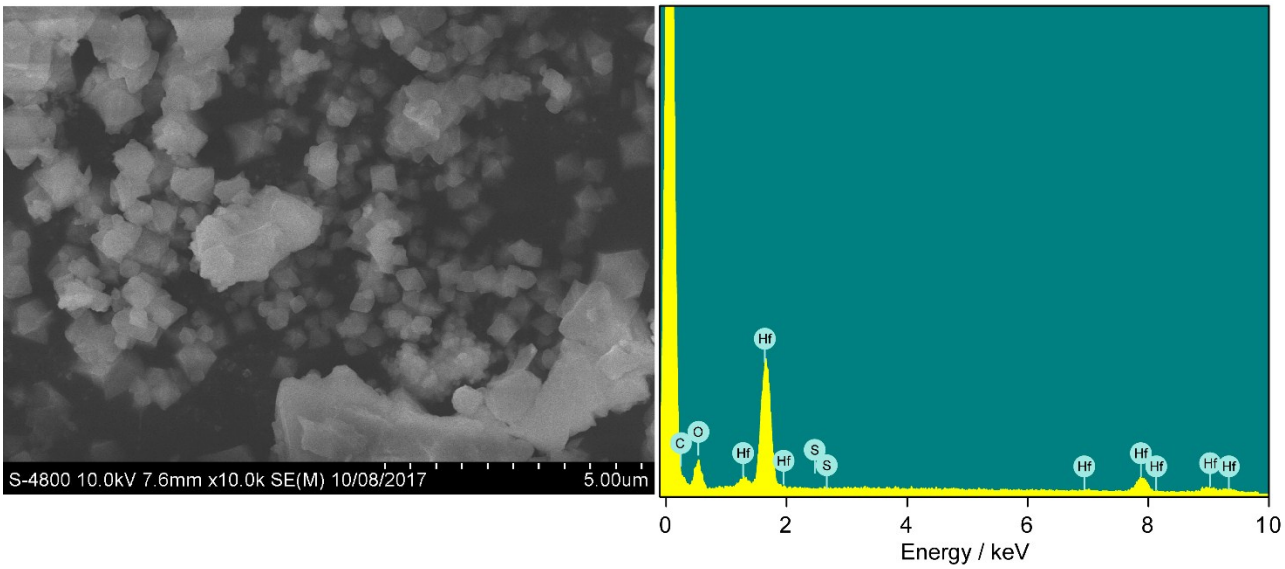

Fig. S13. Scanning electron microscopy (SEM) image and Energy-dispersive X-ray (EDX) spectrum of VNU-11-P-SO_4.

Section S8: Transmission Electron Microscopy

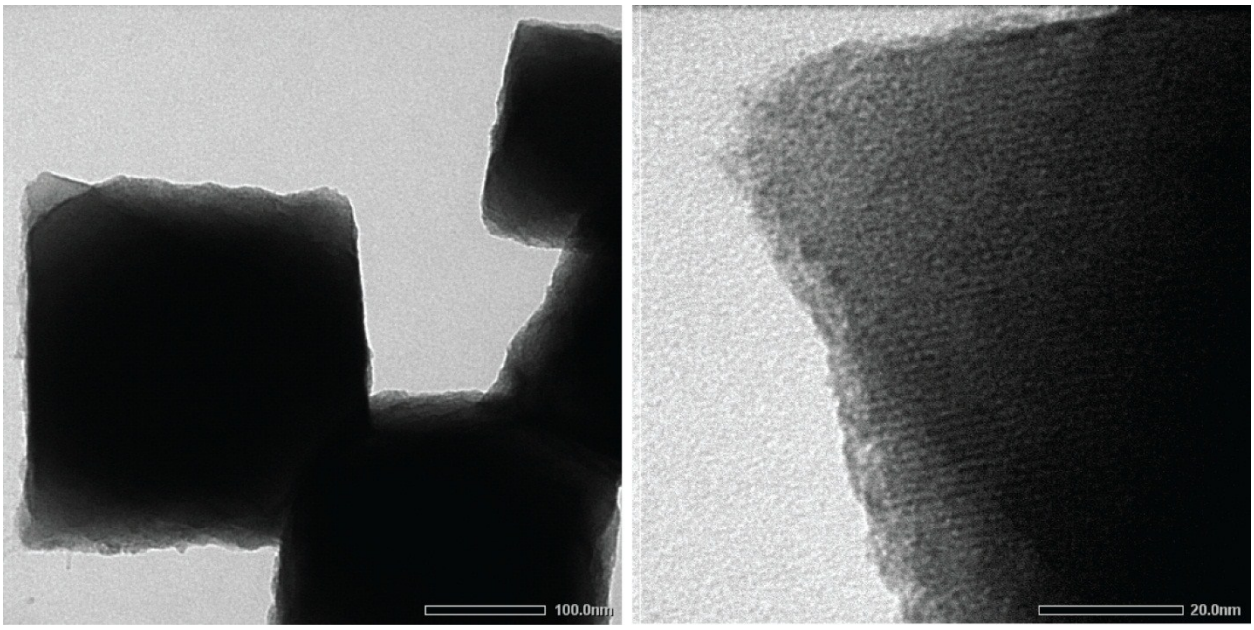

Fig. S14. Transmission electron microscopy (TEM) images of VNU-11-P.

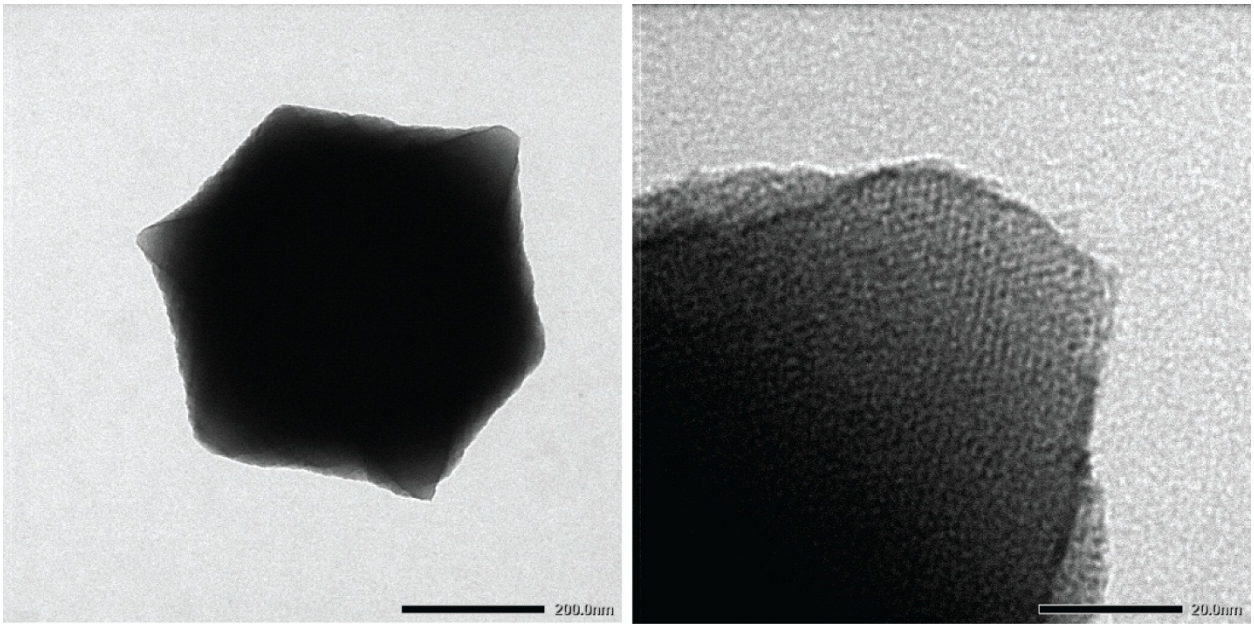

Fig. S15. Transmission electron microscopy (TEM) images of VNU-11-P-SO_4.

Section S9: Catalytic study

An 2-aminophenol (0.119 g, 1 mmol) and benzaldehyde (0.106 g, 1 mmol) were added into a flask pre-charged with VNU-11-P-SO_4 (0.018 g, 0.01 mmol). The reaction was then stirred under solvent-free condition at 140 °C for 6 hour and monitored by TLC. After completion of reaction, the reaction mixture was dissolved in 5 mL acetone, and VNU-11-P-SO_4 catalyst was separated out by centrifugation and washed further with anhydrous acetone (2 × 10 mL) and ethanol (2 × 10 mL). The combined organic layers were evaporated under reduced pressure to obtain the crude product. The crude product was purified by silica gel column chromatography (90:10 acetone/petroleum ether) in order to afford the pure product, which was confirmed via FTIR, ^{1}H-NMR, ^{13}C-NMR, and GC-MS.

Optimization of Catalytic Reaction Conditions

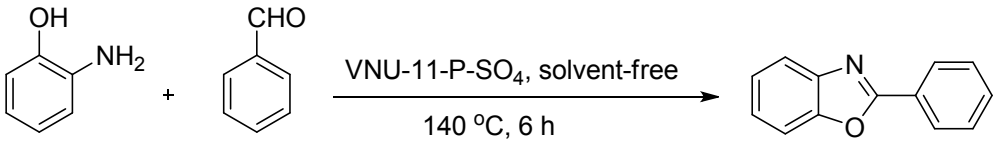

Table S4. Optimization of temperature on the synthesis of 2-phenylbenzoxazole.

Entry	Temperature (°C)	Isolated yield (%)
1	80	25
2	100	29
3	120	62
4	130	78
5	140	99

Table S5. Optimization of reaction time on the synthesis of 2-phenylbenzoxazole.

Entry	Time (h)	Isolated yield (%)
1	1	19
2	2	40
3	3	57
4	4	71
5	5	83
6	6	99
7	7	99

Table S6. Optimization of catalyst ratio on the synthesis of 2-phenylbenzoxazole.

Entry	VNU-11-P-SO_4 (mol%)	Isolated yield (%)
1	0.25	50
2	0.50	62
3	0.75	76
4	1.00	99
5	1.25	98
6	1.50	99

[a]Reaction conditions: A mixture of 2-aminophenol (1 mmol), benzaldehyde (1 mmol), and VNU-11-P-SO_4 was stirred at 140 ^oC for 6 h. [b]Yield of 2-phenylbenzoxazole was isolated by column chromatography (acetone/hexane).

Table S7. Optimization of solvents condition on the synthesis of 2-phenylbenzoxazole.

Entry[a]	Type of solvent	Solvents	Isolated yield (%)[b]
1	Polar protic	Ethanol	85
2		*n*-Butanol	62
3	Polar aprotic	DMF	71
4		THF	37
5	Non polar	Dichloromethane	40
6		Toluene	49
7		1,4-Dioxane	95
8	Free-solvent	-	99

[a]Reaction conditions: A mixture of 2-aminophenol (1 mmol), benzaldehyde (1 mmol), and VNU-11-P-SO_4 (0.01 mmol) was stirred at 140 ^oC for 6 h. [b]Yield of 2-phenylbenzoxazole was isolated by column chromatography (acetone/hexane).

Leaching test for VNU-11-P-SO_4

Reaction time	2.0 h	4.0 h	6.0 h
Isolated yield (%)	40	71	99
Hf^{4+} leaching (ppb)	28	44	48

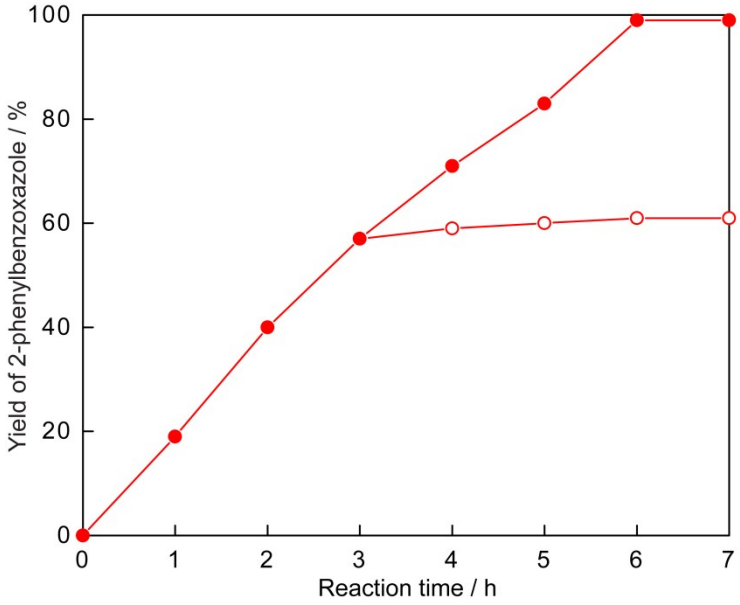

Fig. S16. Leaching test for VNU-11-P-SO_4-catalyzed synthesis of 2-phenylbenzoxazole: after 3 h, the reaction mixture was split in two parts and the catalyst was withdrawn from one sample (red hollow).

Table S8. Comparison of catalysts on the synthesis of 2-phenylbenzoxazole.

Entry	Type of catalysts	Catalyst	Chemical formula	Isolated yield (%)
1	Free-catalyst	-	-	5
2	MOFs	VNU-11-P-SO_4	$Hf_6O_5(OH)_3(BTC)_2(SO_4)_{2.5}$[a]	99
3		VNU-11-P	$Hf_6O_5(OH)_3(BTC)_2(HCOO)_5$	78
4		VNU-1	$Zr_6O_4(OH)_4(CPEB)_6$[b]	68
5		VNU-2	$Hf_6O_4(OH)_4(CPEB)_6$	69
6		UiO-66	$Zr_6O_4(OH)_4(BDC)_6$[c]	49
7		MOF-808-2.5SO_4	$Zr_6O_5(OH)_3(BTC)_2(SO_4)_{2.5}$	83
8		MOF-808-P	$Zr_6O_5(OH)_3(BTC)_2(HCOO)_5$	79
9		MOF-177	$Zn_4O(BTB)_2$[d]	63
10		HKUST-1	$Cu_3(BTC)_2$	63
11		ZIF-8	$Zn(mIm)_2$[e]	34
12	Metal salts	Aluminium chloride	$AlCl_3$	53
13		Iron(III) chloride	$FeCl_3$	41
14		Zinc chloride	$ZnCl_2$	51
15		Copper acetate	$Cu(CH_3COO)_2$	36
16		Hafnium chloride	$HfCl_4$	12
17	Brønsted acids	Sufuric acid	H_2SO_4	35
18		Hydrochloric acid	HCl	22
19		Phosphoric acid	H_3PO_4	25
20		Trifluoroacetic acid	CF_3COOH	33
21		Triflic acid	TsOH	44

[a]BTC = 1,3,5-benzenetricarboxylic; [b]CPEB = 1,4-bis(2-[4-carboxyphenyl]ethynyl)benzene; [c]BDC = 1,4-benzenedicarboxylate; [d]BTB = benzene-1,3,5-tribenzoate; [e]mIm = *N*-methylimidazole.

Recyclability study

For the recycling experiment, the recovered catalyst was washed with anhydrous acetone (3 × 5 mL) and ethanol (3 × 5 mL) before being isolated by centrifugation. The catalyst was then dried under reduced pressure and re-applied to the next cycle.

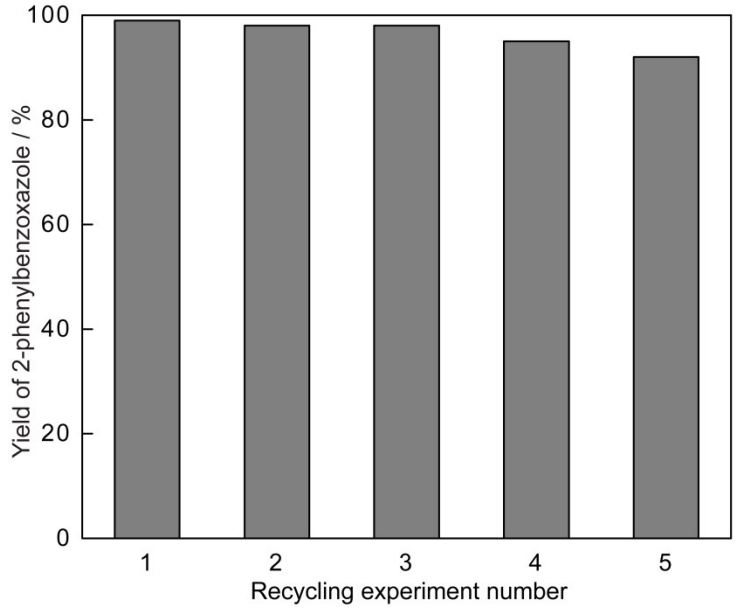

Fig. S17. The recycling experiments of VNU-11-P-SO_4-catalyzed synthesis of 2-phenylbenzoxazole over five cycles.

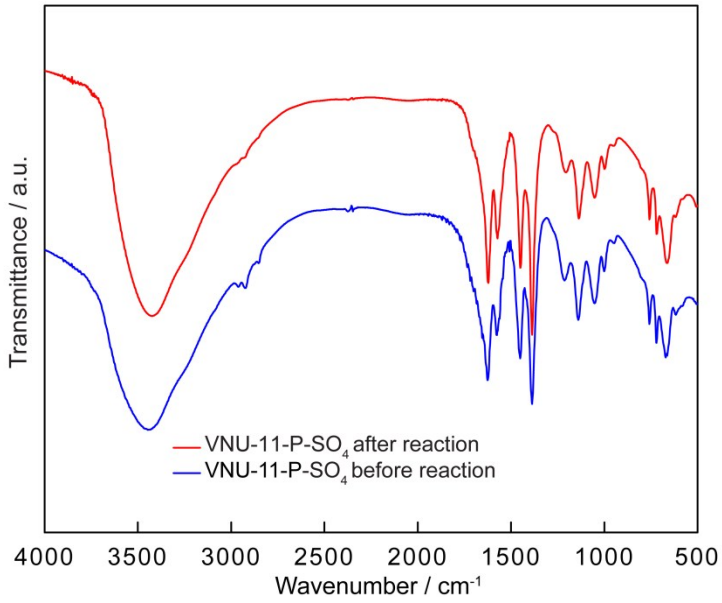

Fig. S18. Infrared spectra of VNU-11-P-SO_4 before (blue) and after (red) synthesis of 2-phenylbenzoxazole.

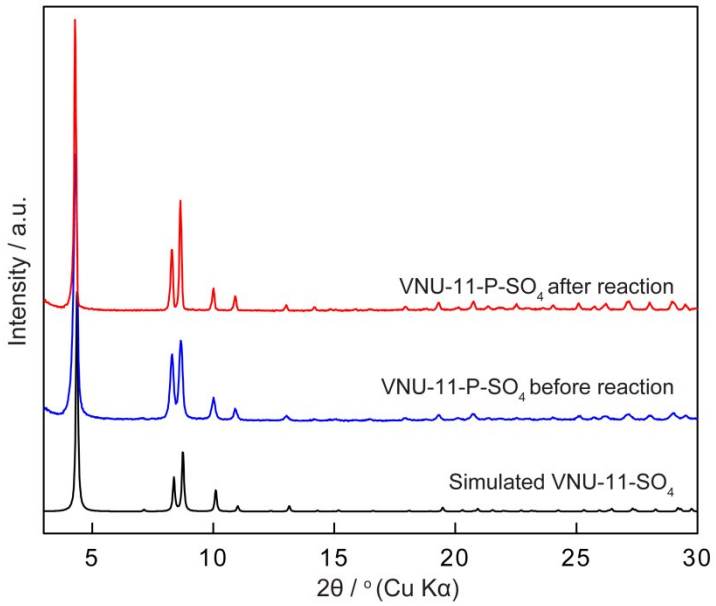

Fig. S19. PXRD analysis of VNU-11-P-SO_4 before (blue) and after (red) synthesis of 2-phenylbenzoxazole in comparison to the simulated pattern.

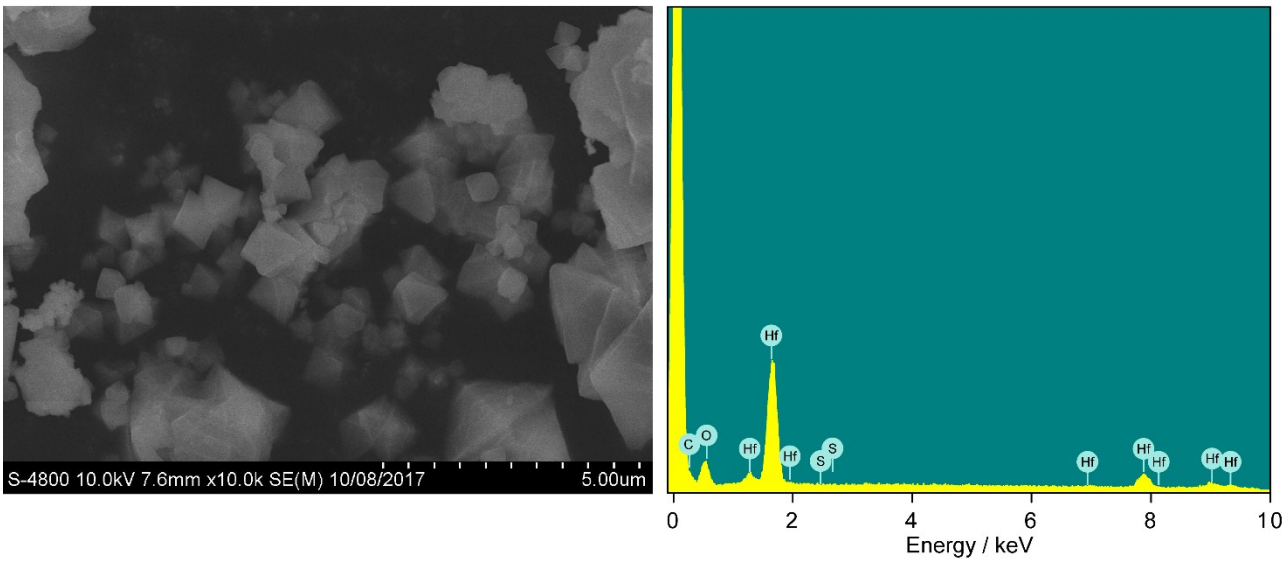

Fig. S20. Scanning electron microscopy (SEM) image and Energy-Dispersive X-ray (EDX) spectrum of VNU-11-P-SO_4 after synthesis of 2-phenylbenzoxazole.

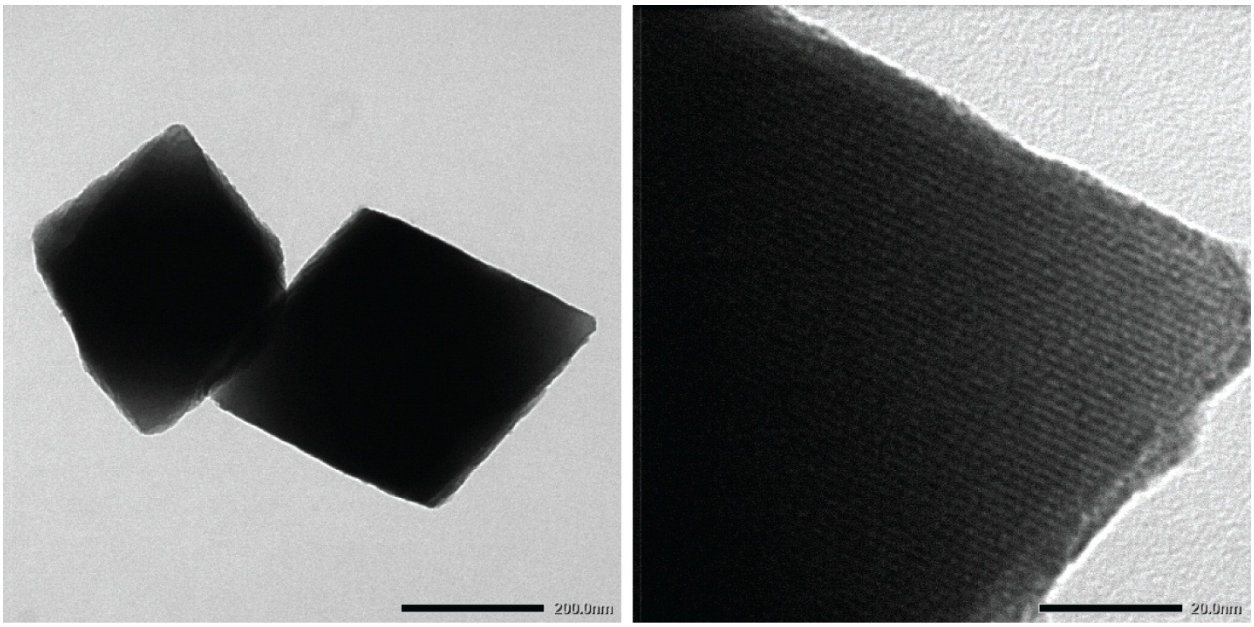

Fig. S21. Transmission electron microscopy (TEM) images of VNU-11-P-SO_4 after synthesis of 2-phenylbenzoxazole.

Table S9. The solvent-free synthesis of benzoxazoles from 2-aminophenols and arylaldehydes catalyzed by VNU-11-P-SO_4 at 140 ^oC.

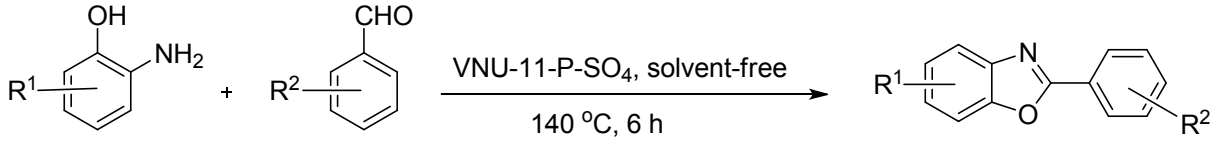

An 2-aminophenol (0.119 g, 1 mmol) and a benzaldehyde derivative (0.106 g, 1 mmol) were added into a flask pre-charged with VNU-11-P-SO_4 (0.018 g, 0.01 mmol). The reaction was then stirred under solvent-free conditions\ at 140 °C for 6-7 hours and monitored by TLC. After completion of reaction, the reaction mixture was dissolved in 5 mL acetone, and VNU-11-P-SO_4 catalyst was separated out by centrifugation and washed further with ecetone (2 × 10 mL) and ethanol (2 × 10 mL). The combined organic layers were evaporated under reduced pressure to obtain the crude product. The crude product was purified by silica gel column chromatography (90:10 acetone/petroleum ether) in order to afford the pure product, which was confirmed via FTIR, ^{1}H-NMR, ^{13}C-NMR, and GC-MS.

Entry	2-Aminophenol	Benzaldehyde	Products	Condi-tions	Isolated yield (%)
1	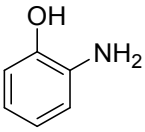	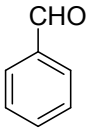	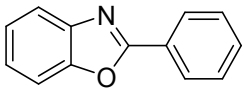	140 °C 6 h	95
2	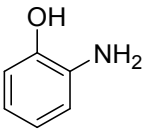	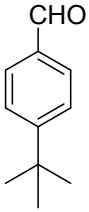	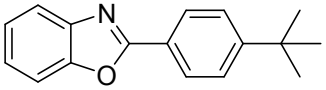	140 °C 6 h 30 m	91
3	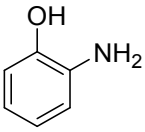	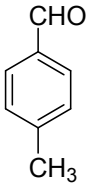	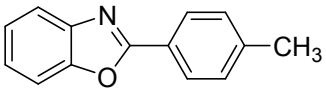	140 °C 6 h	90
4	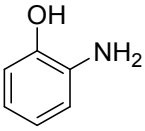	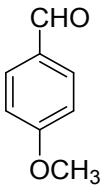	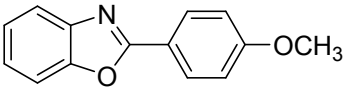	140 °C 6 h	88

5	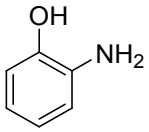	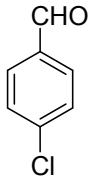	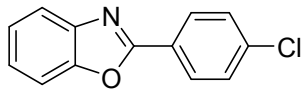	140 °C 7 h	85
6	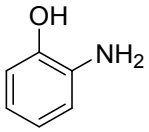	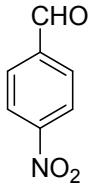	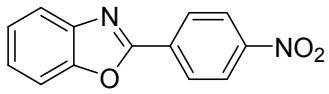	140 °C 5.5 h	89
7	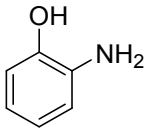	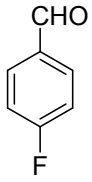	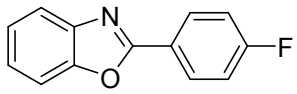	140 °C 5.5 h	87
8	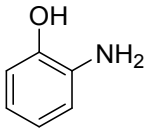	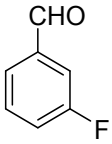	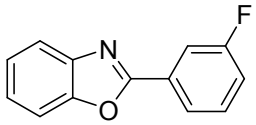	140 °C 5 h	90
9	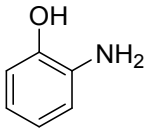	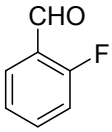	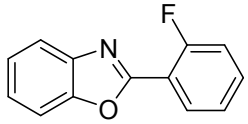	140 °C 5 h	92
10	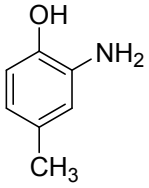	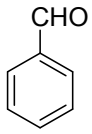	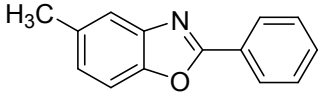	140 °C 5 h	87
11	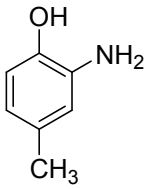	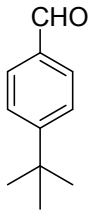	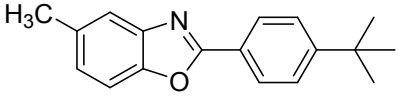	140 °C 6.5 h	90
12	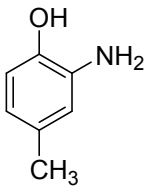	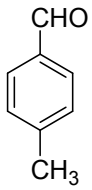	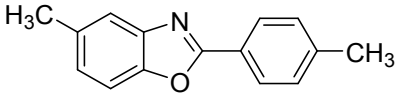	140 °C 5.5 h	92
13	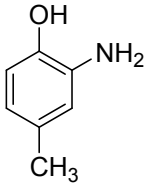	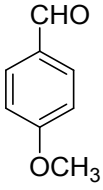	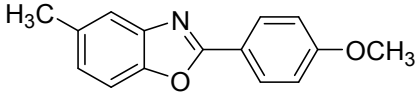	140 °C 5.5 h	85

14	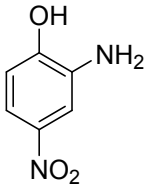	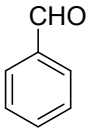	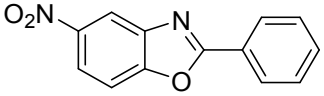	140 °C 6 h	90
15	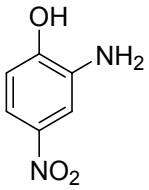	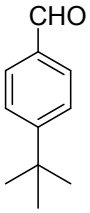	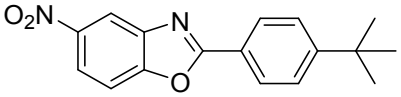	140 °C 6.5 h	87
16	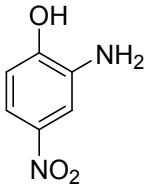	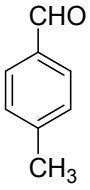	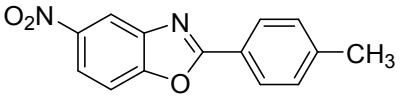	140 °C 6 h	87
17	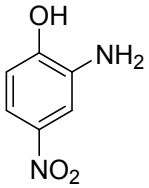	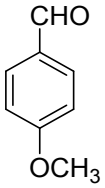	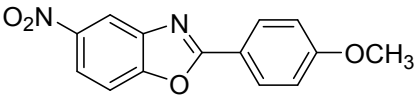	140 °C 5 h	91
18	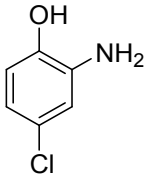	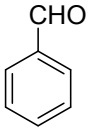	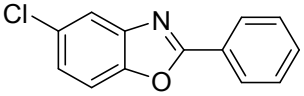	140 °C 6 h	90
19	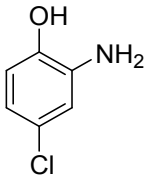	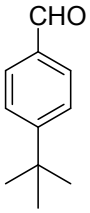	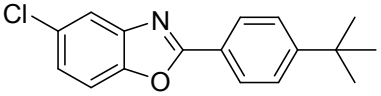	140 °C 6 h	95
20	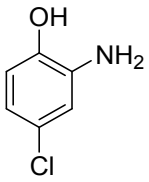	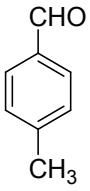	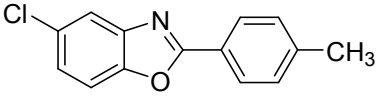	140 °C 5 h	86
21	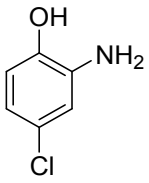	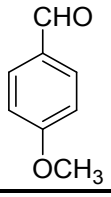	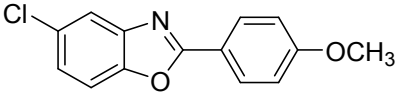	140 °C 5 h	85

Section S10: Characterization of 2-Aryl Substituted Benzoxazoles

2-Phenylbenzoxazole

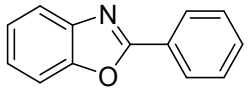

Melting point: 102-103.5 °C

FT-IR (KBr, 4000-400 cm^{-1}): 3059, 2925, 2854, 1775, 1615, 1551, 1475, 1448, 1285, 1240.

^1H NMR (500 MHz, $CDCl_3$) δ 8.31-8.22 (m, 2H), 7.82-7.75 (m, 1H), 7.61-7.56 (m, 1H), 7.55-7.50 (m, 3H), 7.40-7.33 (m, 2H).

^{13}C NMR (125 MHz, $CDCl_3$) δ 163.2, 150.9, 142.2, 131.7, 129.0, 127.8, 127.3, 125.3, 124.7, 120.1, 110.7.

2-(4-*tert*-Butylphenyl)benzoxazole

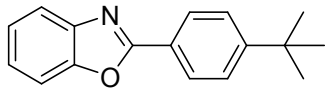

Melting point: 107-108 °C

FT-IR (KBr, 4000-400 cm^{-1}): 3059, 2927, 1728, 1547, 1452, 1429, 1287, 1239.

^1H NMR (500 MHz, $CDCl_3$) δ 8.21-8.16 (m, 2H), 7.75-7.78 (m, 1H), 7.60-7.56 (m, 1H), 7.56-7.54 (m, 2H), 7.37-7.32 (m, 2H), 1.38 (s, 9H).

^{13}C NMR (125 MHz, $CDCl_3$) δ 163.4, 155.4, 150.8, 142.1, 127.7, 126.1, 125.1, 124.7, 124.4, 120.0, 110.7, 35.2, 31.3.

2-(*p*-Tolyl)benzoxazole

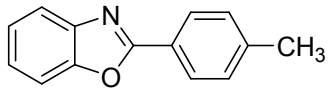

Melting point: 113-114.5 °C

FT-IR (KBr, 4000-400 cm^{-1}): 3056, 2920, 2854, 1728, 1620, 1554, 1499, 1450, 1242.

^1H NMR (500 MHz, $CDCl_3$) δ 8.17-8.13 (m, 2H), 7.74-7.77 (m, 1H), 7.50-7.58 (m, 1H), 7.35-7.31 (m, 4H), 2.44 (s, 3H).

^{13}C NMR (125 MHz, $CDCl_3$) δ 163.5, 150.8, 142.3, 142.2, 129.8, 127.8, 125.1, 124.7, 124.5, 120.0, 110.6, 21.8.

2-(4-Methoxyphenyl)benzoxazole

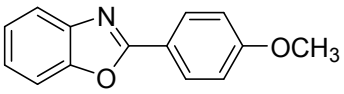

Melting point: 103-104.5 °C

FT-IR (KBr, 4000-400 cm^{-1}): 3050, 2924, 2849, 1615, 1501, 1450, 1420, 1244.

^1H NMR (500 MHz, $CDCl_3$) δ 8.23-8.17 (m, 2H), 7.75-7.73 (m, 1H), 7.54-7.56 (m, 1H), 7.35-7.29 (m, 2H), 7.05-7.01 (m, 2H), 3.89 (s, 3H).

^{13}C NMR (125 MHz, $CDCl_3$) δ 163.3, 162.6, 150.8, 142.1, 129.7, 124.8, 124.7, 119.7, 119.7, 114.6, 110.6, 55.6.

2-(4-Chlorophenyl)benzoxazole

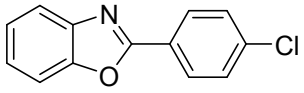

Melting point: 148-150 °C

FT-IR (KBr, 4000-400 cm^{-1}): 3067, 2922, 1725, 1607, 1451, 1428, 1237.

^1H NMR (500 MHz, CD_3CO) δ 8.26-8.22 (m, 2H), 7.77-7.75 (m, 1H), 7.70-7.69 (m, 1H), 7.65-7.62 (m, 2H), 7.42 (pd, J = 7.5, 2.0 Hz, 2H).

^{13}C NMR (125 MHz, CD_3CO) δ 161.7, 150.8, 142.1, 137.2, 129.3, 129.0, 125.9, 125.6, 124.9, 120.0, 110.7.

2-(4-Nitrophenyl)benzoxazole

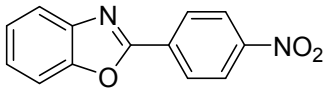

Melting point: 156-157 °C

FT-IR (KBr, 4000-400 cm^{-1}): 2925, 2854, 1678, 1610, 1534, 1449, 1237.

^1H NMR (500 MHz, $CDCl_3$) δ 8.15 (dd, J = 8.0, 1.0 Hz, 1H), 7.89 (dd, J = 8.0, 1.0 Hz, 1H), 7.83-7.80 (m, 1H), 7.74 (td, J = 8.0, 1.0 Hz, 1H), 7.69 (td, J = 8.0, 1.0 Hz, 1H), 7.59-7.57 (m, 1H), 7.42-7.37 (m, 2H).

^{13}C NMR (125 MHz, $CDCl_3$) δ 158.9, 151.2, 141.7, 132.4, 132.0, 131.6, 126.2, 125.1, 124.3, 121.7, 120.9, 111.1.

2-(4-Fluorophenyl)benzoxazole

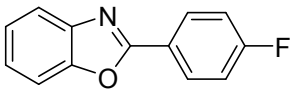

Melting point: 99-99.5 °C

FT-IR (KBr, 4000-400 cm^{-1}): 3061, 2925, 1619, 1584, 1582, 1542, 1473, 1448, 1247, 1225.

^{1}H NMR (500 MHz, $CDCl_3$) δ 8.30-8.22 (m, 2H), 7.80-7.72 (m, 1H), 7.60-7.53 (m, 1H), 7.40-7.32 (m, 2H), 7.23-7.17 (m, 2H).

^{13}C NMR (125 MHz, $CDCl_3$) δ 165.98 (s), 163.97 (s), 162.32 (s), 150.94 (s), 142.22 (s), 131.03 (s), 129.99 (d, J = 8.8 Hz), 128.99 (s), 125.28 (s), 124.81 (s), 123.67 (d, J = 3.2 Hz), 120.14 (s), 116.41 (s), 116.24 (s), 110.70 (s).

2-(3-Fluorophenyl)benzoxazole

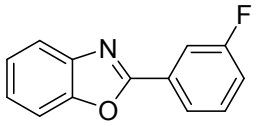

Melting point: 99-100 °C

FT-IR (KBr, 4000-400 cm^{-1}): 3073, 2925, 2855, 1591, 1552, 1480, 1449, 1341, 1269, 1242.

^{1}H NMR (500 MHz, $CDCl_3$) δ 8.05 (dd, J = 8.0, 1.0 Hz, 1H), 7.95 (dd, J = 8.5, 1.0 Hz, 1H), 7.79-7.77 (m, 1H), 7.59-7.58 (m, 1H), 7.49 (dd, J = 13.5, 8.0 Hz, 1H), 7.40-7.35 (m, 2H), 7.25-7.20 (m, 1H).

^{13}C NMR (125 MHz, $CDCl_3$) δ 164.1 (s), 162.1 (s), 150.9 (s), 142.1 (s), 130.76 (d, J = 8.1 Hz), 129.35 (d, J = 8.6 Hz), 125.6 (s), 124.9 (s), 123.5 (d, J = 3.0 Hz), 120.4 (s), 118.63 (d, J = 21.3) 114.70 (d, J = 23.9), 110.8 (s).

2-(2-Fluorophenyl)benzoxazole

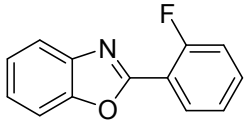

Melting point: 93-95 °C

FT-IR (KBr, 4000-400 cm^{-1}): 2923, 1664, 1582, 1550, 1447, 1245.

^{1}H NMR (500 MHz, $CDCl_3$) δ 8.24 (td, *J* = 7.5, 2.0 Hz, 1H), 7.85-7.81(m, 1H), 7.63-7.59 (m, 1H), 7.54-7.49 (m, 1H), 7.41-7.36 (m, 2H), 7.32-7.25 (m, 2H).

^{13}C NMR (125 MHz, $CDCl_3$) δ 162.0 (s), 156.0(s), 150.7 (s), 141.9 (s), 133.25 (d, *J* = 8.6 Hz), 130.7 (d, *J* = 1.1 Hz), 125.6 (s), 124.8 (s), 124.63 (d, *J* = 3.8 Hz), 120.52 (s), 117.32 (d, *J* = 21.3 Hz), 115.7 (d, *J* = 10.4 Hz), 110.8 (s).

5-Methyl-2-phenylbenzoxazole

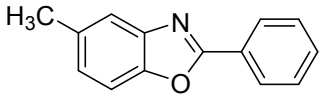

Melting point: 112-115 °C

FT-IR (KBr, 4000-400 cm^{-1}): 2918, 1626, 1552, 1445, 1263.

^{1}H NMR (500 MHz, $(CD_3)_2CO$) δ 8.25-8.23 (m, 2H), 7.62-7.59 (m, 3H), 7.57-7.56 (m, 2H), 7.24 (d, *J* = 8.5, 1H), 2.47 (s, 3H).

^{13}C NMR (125 MHz, $CDCl_3$) δ 163.3, 149.2, 142.5, 134.5, 131.5, 129.0, 127.7, 127.5, 126.4, 120.1, 110.1, 21.6.

5-Methyl-2-(4-*tert*-butylphenyl)benzoxazole

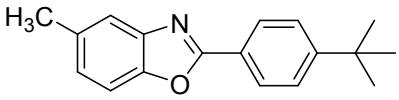

Melting point: 137-140 °C

FT-IR (KBr, 4000-400 cm^{-1}): 3107, 2963, 2930, 2871, 1729, 1621, 1532, 1460, 1269.

^{1}H NMR (500 MHz, $(CD_3)_2CO$) *δ* 8.56 (d, *J* = 2.0 Hz, 1H), 8.34 (dd, *J* = 9.0, 2.0 Hz, 1H), 8.20 (d, *J* = 8.5 Hz, 2H), 7.92 (d, *J* = 9.0 Hz, 1H), 7.69 (d, *J* = 9.0 Hz, 2H), 2.81 (s, 3H), 1.39 (s, 9H).

^{13}C NMR (125 MHz, $(CD_3)_2CO$) *δ* 162.9, 155.0, 149.0, 142.5, 134.3, 127.2, 126.1, 126.0, 124.6, 119.7, 109.9, 34.7, 30.5, 20.5.

5-Methyl-2-(*p*-tolyl)benzoxazole

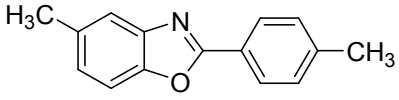

Melting point: 135 °C.

FT-IR (KBr, 4000 – 400 cm^{-1}): 3304, 2921, 2856, 1616, 1555, 1499, 1332, 1262.

^{1}H NMR (500 MHz, $(CD_3)_2CO$) δ 8.11 (d, J = 8.0 Hz, 2H), 7.53 – 7.51 (m, 2H), 7.39 (d, J = 8.0 Hz, 2H), 7.22 – 7.19 (m, 1H), 2.46 (s, 3H), 2.43 (s, 3H).

^{13}C NMR (125 MHz, $(CD_3)_2CO$) δ 163.2, 149.2, 142.7, 142.3, 134.5, 129.9, 127.5, 126.3, 124.8, 119.9, 110.1, 20.9, 20.8.

5-Methyl-2-(4-methoxyphenyl)benzoxazole

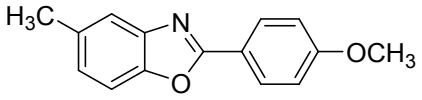

Melting point: 112 °C

FT-IR (KBr, 4000 – 400 cm^{-1}): 2924, 2854, 1730, 1608, 1499, 1420, 1254.

^{1}H NMR (500 MHz, DMSO) δ 8.12 (d, J = 9.0 Hz, 2H), 7.61 (d, J = 8.0 Hz, 1H), 7.55 (s, 1H), 7.20 (d, J = 8.5 Hz, 1H), 7.15 (d, J = 9.0 Hz, 2H), 3.87 (s, 3H), 2.44 (s, 3H).

^{13}C NMR (125 MHz, DMSO) δ 163.0, 162.5, 148.7, 142.1, 134.7, 129.5, 126.5, 119.6, 119.5, 119.2, 115.2, 110.6, 110.5, 55.9, 21.3.

5-Nitro-2-phenylbenzoxazole

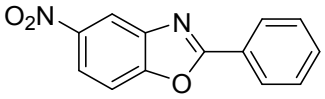

Melting point: 166-169 °C.

FT-IR (KBr, 4000-400 cm^{-1}): 3105, 2925, 2853, 1709, 1604, 1526, 1463, 1348, 1286.

^{1}H NMR (500 MHz, DMSO-d_6) δ 8.68 (d, J = 2.5 Hz, 1H), 8.35 (dd, J = 9.0, 2.0 Hz, 1H), 8.26-8.24 (m, 2H), 8.06 (d, J = 9.0 Hz, 1H), 7.71-7.65 (m, 3H).

^{13}C NMR (125 MHz, $CDCl_3$) δ 165.4 (s), 154.0 (s), 145.1 (s), 141.9 (s), 132.9 (s), 129.5 (s), 127.8 (d, J = 14.3 Hz), 125.5 (s), 121.5 (d, J = 16.8 Hz), 115.7 (d, J = 12.5 Hz), 111.8 (s).

5-Nitro-2-(4-*tert*-butylphenyl)benzoxazole

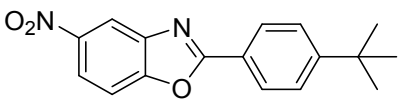

Melting point: 137 °C.

FT-IR (KBr, 4000-400 cm^{-1}): 3106, 2964, 2869, 1724, 1619, 1531, 1496, 1462, 1343, 1267.

^{1}H NMR (500 MHz, $(CD_3)_2CO$) δ 8.18-8.16 (m, 2H), 7.66-7.63 (m, 2H), 7.56-7.54 (m, 2H), 7.23-7.21 (m, 1H), 1.38 (s, 9H).

^{13}C NMR (125 MHz, $(CD_3)_2CO$) δ 166.9, 157.3, 155.3, 146.4, 143.6, 132.1, 129.7, 128.7, 127.2, 124.2, 122.0, 116.4, 112.1, 35.8, 31.4.

5-Nitro-2-(*p*-tolyl)benzoxazole

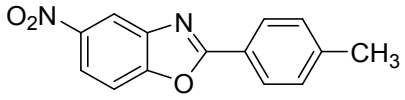

Melting point: 125-126 ^{o}C.

FT-IR (KBr, 4000-400 cm^{-1}): 2923, 2850, 1695, 1628, 1515, 1416, 1328, 1250.

^{1}H NMR (500 MHz, $(CD_3)_2CO$) δ 8.31-8.27 (m, 2H), 7.57-7.55 (m, 2H), 7.40-7.35 (m, 2H), 7.24 (d, J = 9.0 Hz, 1H), 2.47 (s, 3H).

^{13}C NMR (125 MHz, $(CD_3)_2CO$) δ 166.7, 164.7, 150.0, 143.3, 135.5, 130.8, 130.7, 127.30, 124.8, 120.7, 117.2, 117.0, 110.9, 21.4.

5-Nitro-2-(4-methoxyphenyl)benzoxazole

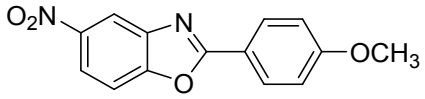

Melting point: 182-186 ^{o}C.

FT-IR (KBr, 4000-400 cm^{-1}): 2923, 2854, 1620, 1628, 1524, 1460, 1343, 1251.

^{1}H NMR (500 MHz, $(CD_3)_2CO$) δ 8.55 (d, J = 2.5 Hz, 1H), 8.34 (dd, J = 9.0, 2.5 Hz, 1H), 8.25-8.23 (m, 2H), 7.91 (d, J = 9.0 Hz, 1H), 7.20-7.18 (m, 2H), 3.95 (s, 3H).

^{13}C NMR (125 MHz, $(CD_3)_2CO$) δ 163.5, 154.4, 142.8, 129.8, 120.8, 118.3, 115.2, 114.8, 111.0, 55.2.

5-Chloro-2-phenylbenzoxazole

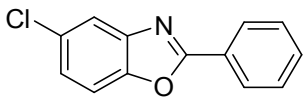

Melting point: 102-104 ^{o}C.

FT-IR (KBr, 4000-400 cm^{-1}): 3061, 1612, 1551, 1443, 1333, 1265.

^{1}H NMR (500 MHz, $(CD_3)_2CO$) δ 8.23 (d, J = 7.5 Hz, 2H), 7.77 (d, J = 1.5 Hz, 1H), 7.70 (d, J = 7.5 Hz, 1H), 7.59-7.64 (m, 3H), 7.42 (dd, J = 9.0, 1.5 Hz, 1H).

^{13}C NMR (125MHz, $(CD_3)_2CO$) δ 165.3, 150.6, 144.5, 133.1, 130.7, 130.2, 128.6, 127.7, 126.4, 120.7, 112.9.

5-Chloro-2-(4-*tert*-butylphenyl)benzoxazole

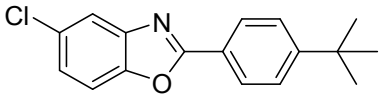

Melting point: 138 ^{o}C

FT-IR (KBr, 4000-400 cm^{-1}): 2957, 2902, 2866, 1611, 1552, 1493, 1457, 1262.

^{1}H NMR (500 MHz, $(CD_3)_2CO$) δ 8.17 (d, J = 8.5 Hz, 2H), 7.76 (s, 1H), 7.70 (d, J = 8.5 Hz, 1H), 7.66 (d, J = 8.5 Hz, 2H), 7.41 (dd, J = 8.5, 2.0 Hz, 1H), 1.38 (s, 9H).

^{13}C NMR (126 MHz, $(CD_3)_2CO$) δ 165.5, 156.7, 150.6, 144.6, 130.6, 128.6, 127.2, 126.2, 125.0, 120.5, 112.8, 35.9, 31.5.

5-Chloro-2-(*p*-tolyl)benzoxazole

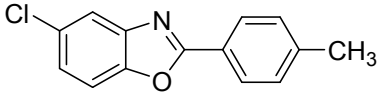

Melting point: 148-150 ^{o}C

FT-IR (KBr, 4000-400 cm^{-1}): 1610, 1551, 1479, 1448, 1258.

^{1}H NMR (500 MHz, $(CD_3)_2CO$) δ 8.13 (d, J = 8.0 Hz, 2H), 7.75 (d, J = 2.0 Hz, 1H), 7.70 (d, J = 9.0 Hz, 1H), 7.40-7.33 (m, 4H), 2.44 (s, 3H).

^{13}C NMR (125 MHz, $(CD_3)_2CO$) δ 165.6, 150.5, 144.6, 143.8, 130.8, 130.6, 128.6, 126.2, 125.0, 120.5, 112.8, 21.7.

5-Chloro-2-(4-methoxyphenyl)benzoxazole

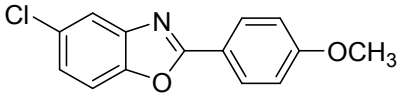

Melting point: 153-155 ^{o}C

FT-IR (KBr, 4000-400 cm^{-1}): 2962, 1609, 1554, 1496, 1451, 1417, 1251.

^{1}H NMR (500 MHz, $(CD_3)_2CO$) δ 8.19-8.17 (m, 2H), 7.72 (d, J = 2.0 Hz, 1H), 7.67 (d, J = 8.5 Hz, 1H), 7.38 (dd, J = 8.5, 2.0 Hz, 1H), 7.16-7.14 (m, 2H), 3.92 (s, 3H).

^{13}C NMR (125 MHz, $(CD_3)_2CO$) δ 165.52, 164.09, 150.53, 144.79, 130.52, 126.57, 125.84, 120.28, 120.04, 115.66, 112.61, 56.16.

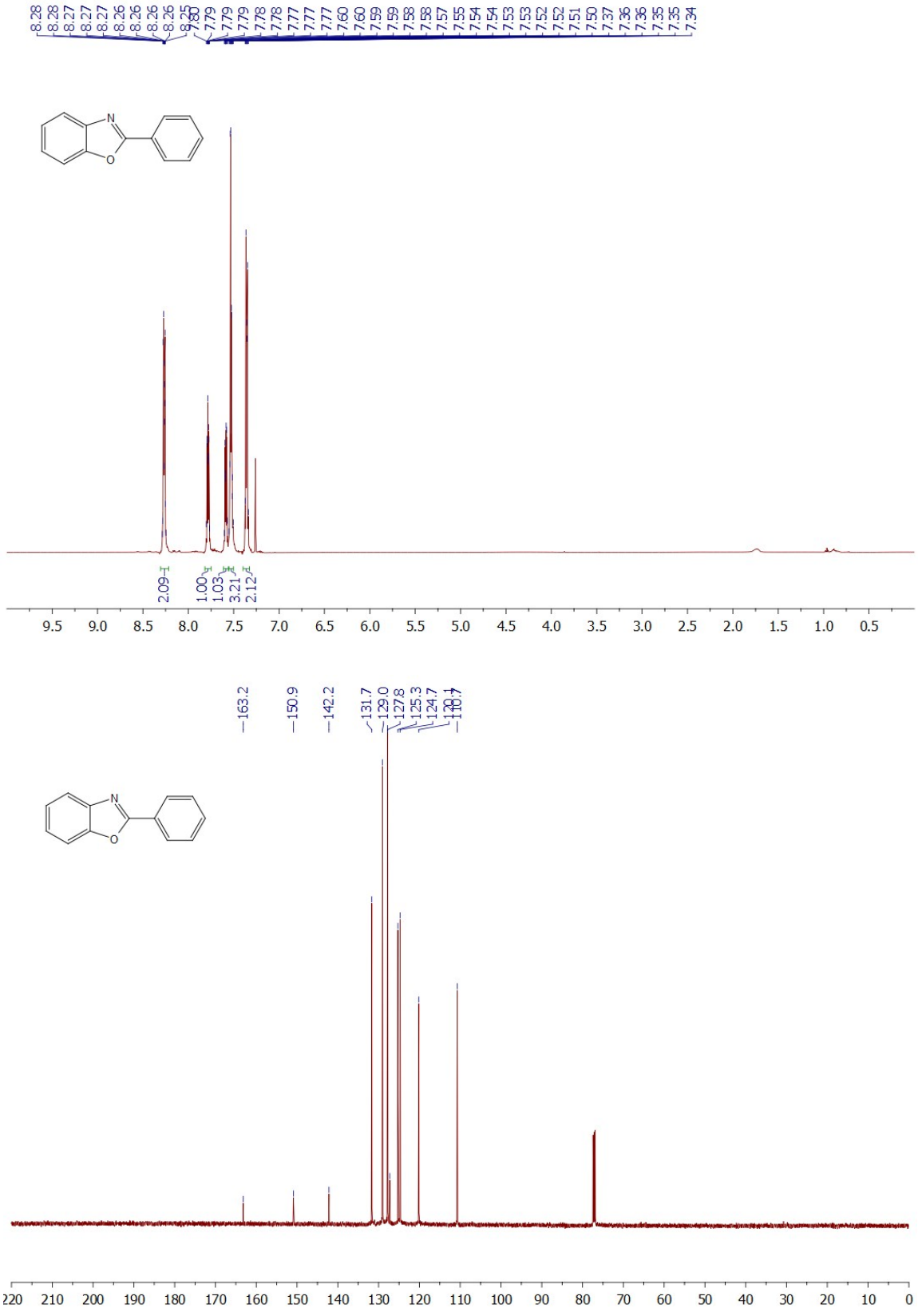

Fig. S22. ^{1}H (top) and ^{13}C (bottom) NMR spectra of 2-phenylbenzoxazole.

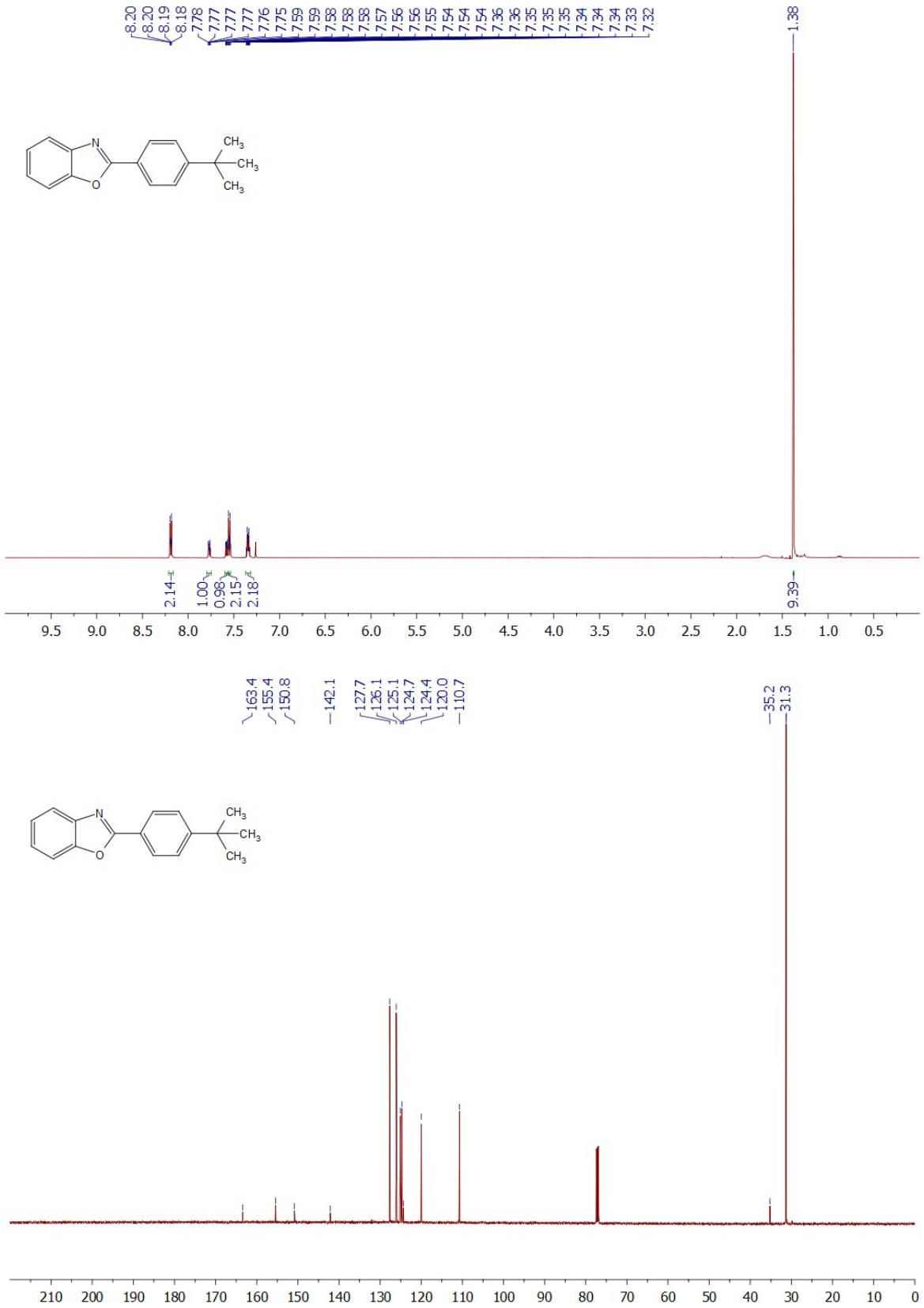

Fig. S23. ^{1}H (top) and ^{13}C (bottom) NMR spectra of 2-(4-*tert*-butylphenyl)benzoxazole.

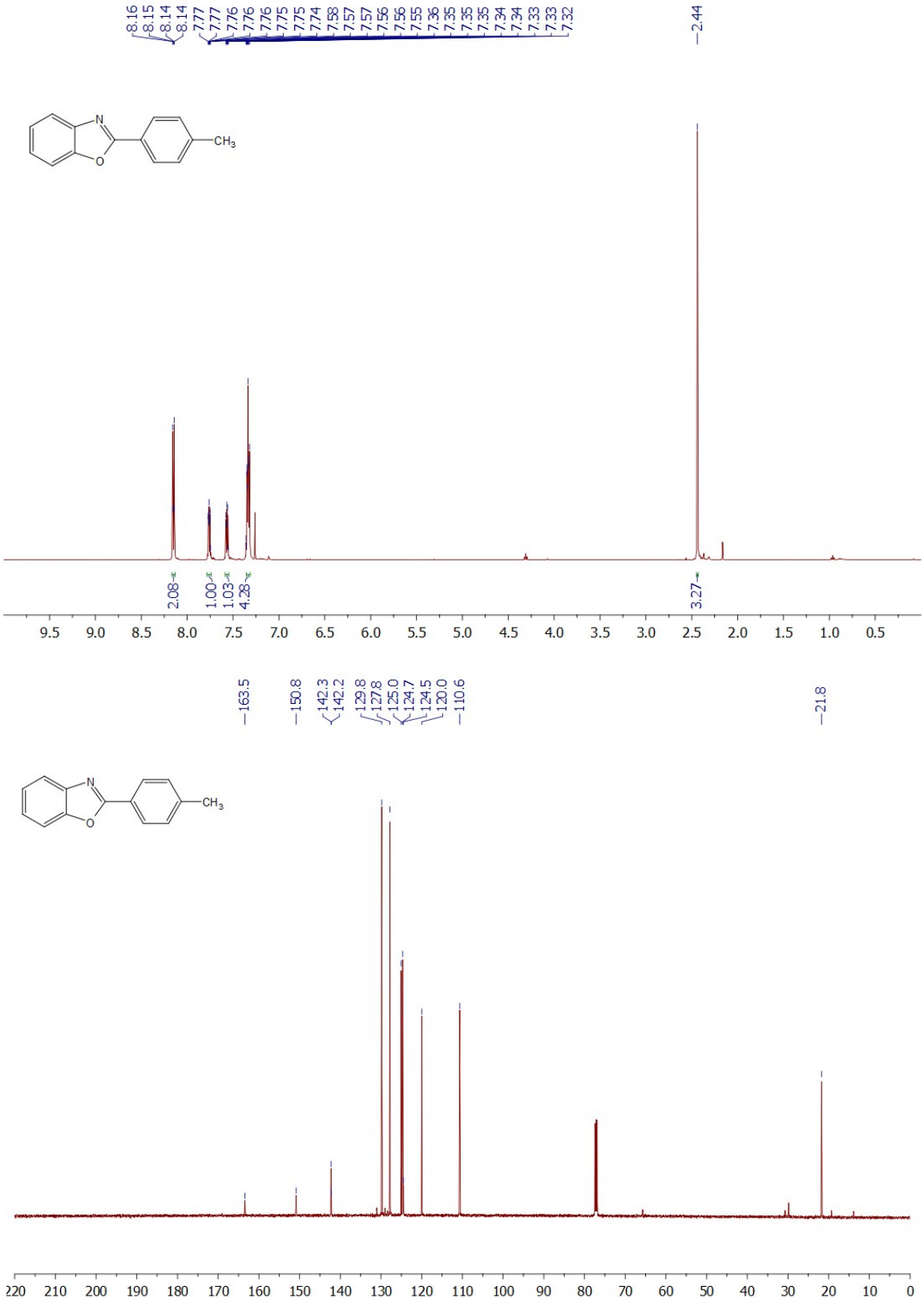

Fig. S24. ^{1}H (top) and ^{13}C (bottom) NMR spectra of 2-(*p*-tolyl)benzoxazole.

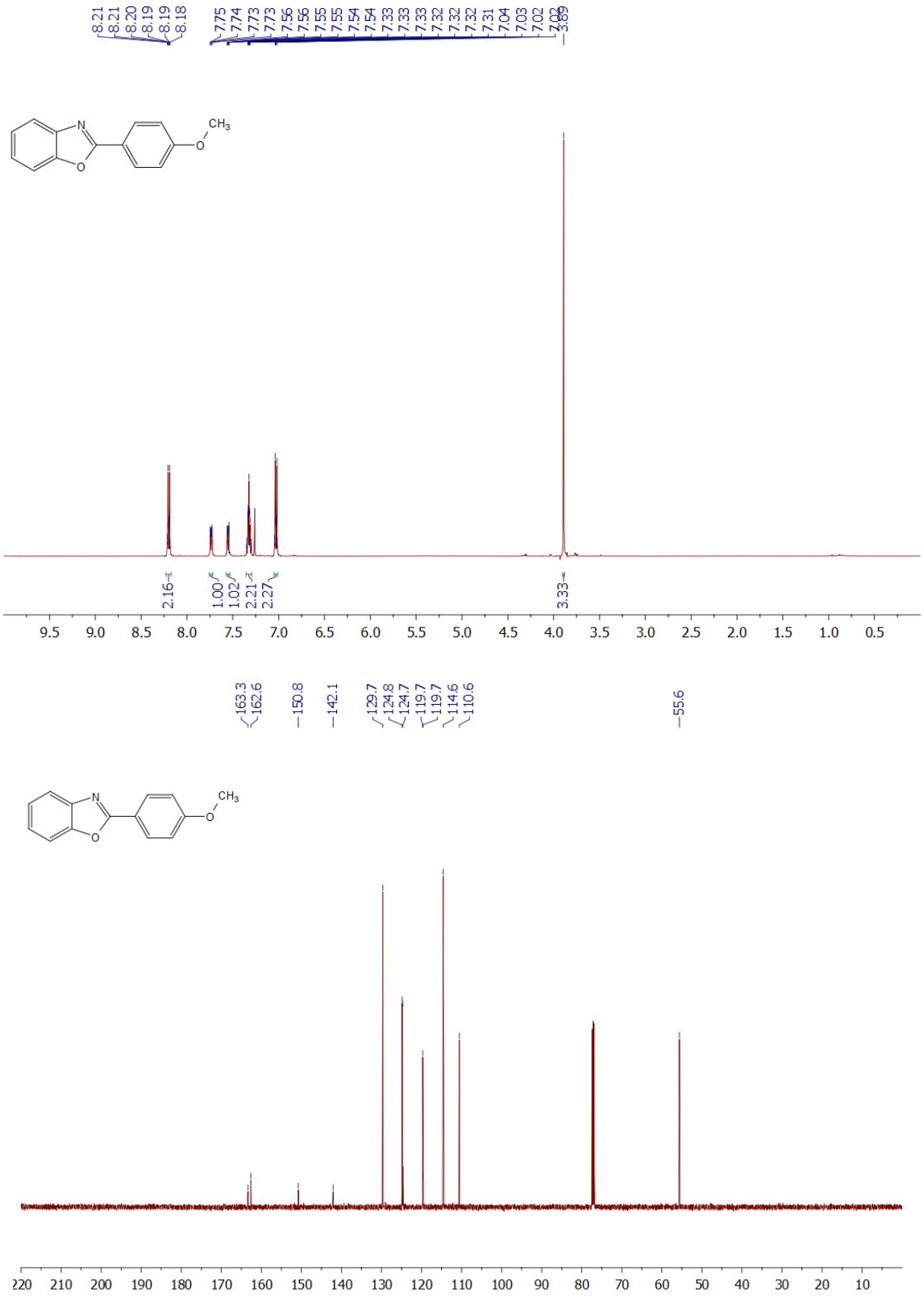

Fig. S25. ^{1}H (top) and ^{13}C (bottom) NMR spectra of 2-(4-methoxyphenyl)benzoxazole.

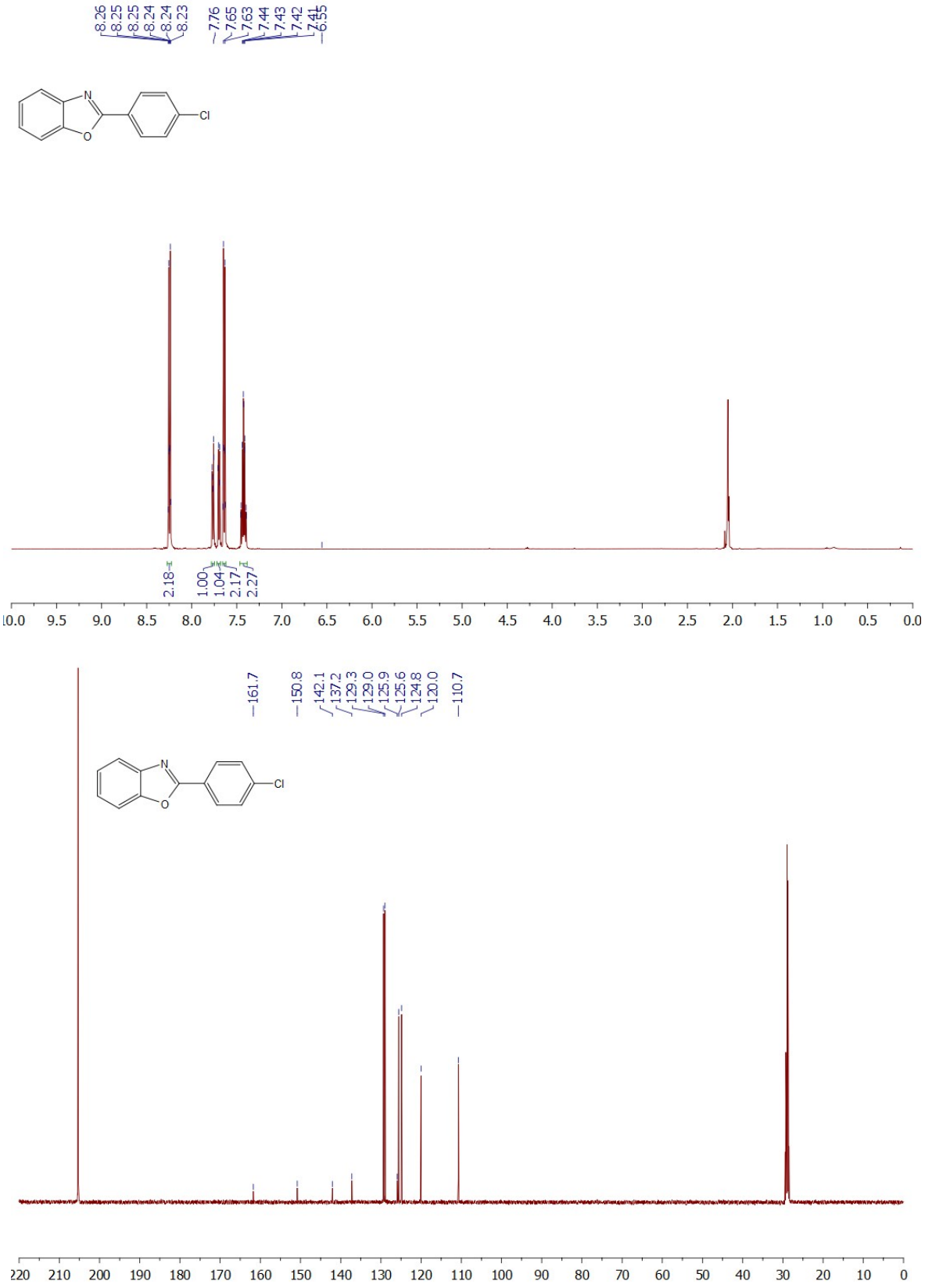

Fig. S26. ^{1}H (top) and ^{13}C (bottom) NMR spectra of 2-(4-chlorophenyl)benzoxazole.

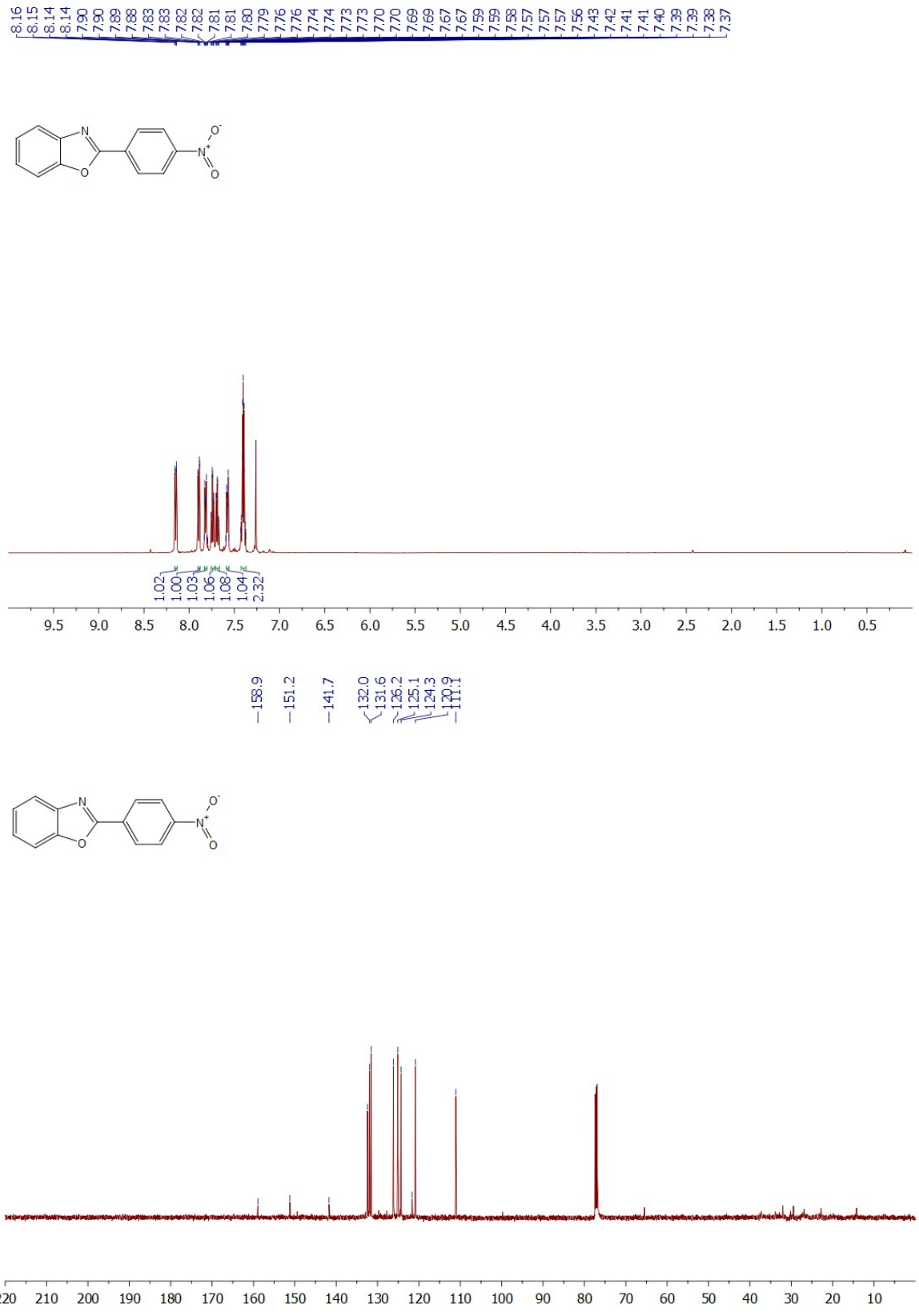

Fig. S27. ^{1}H (top) and ^{13}C (bottom) NMR spectra of 2-(4-nitrophenyl)benzoxazole.

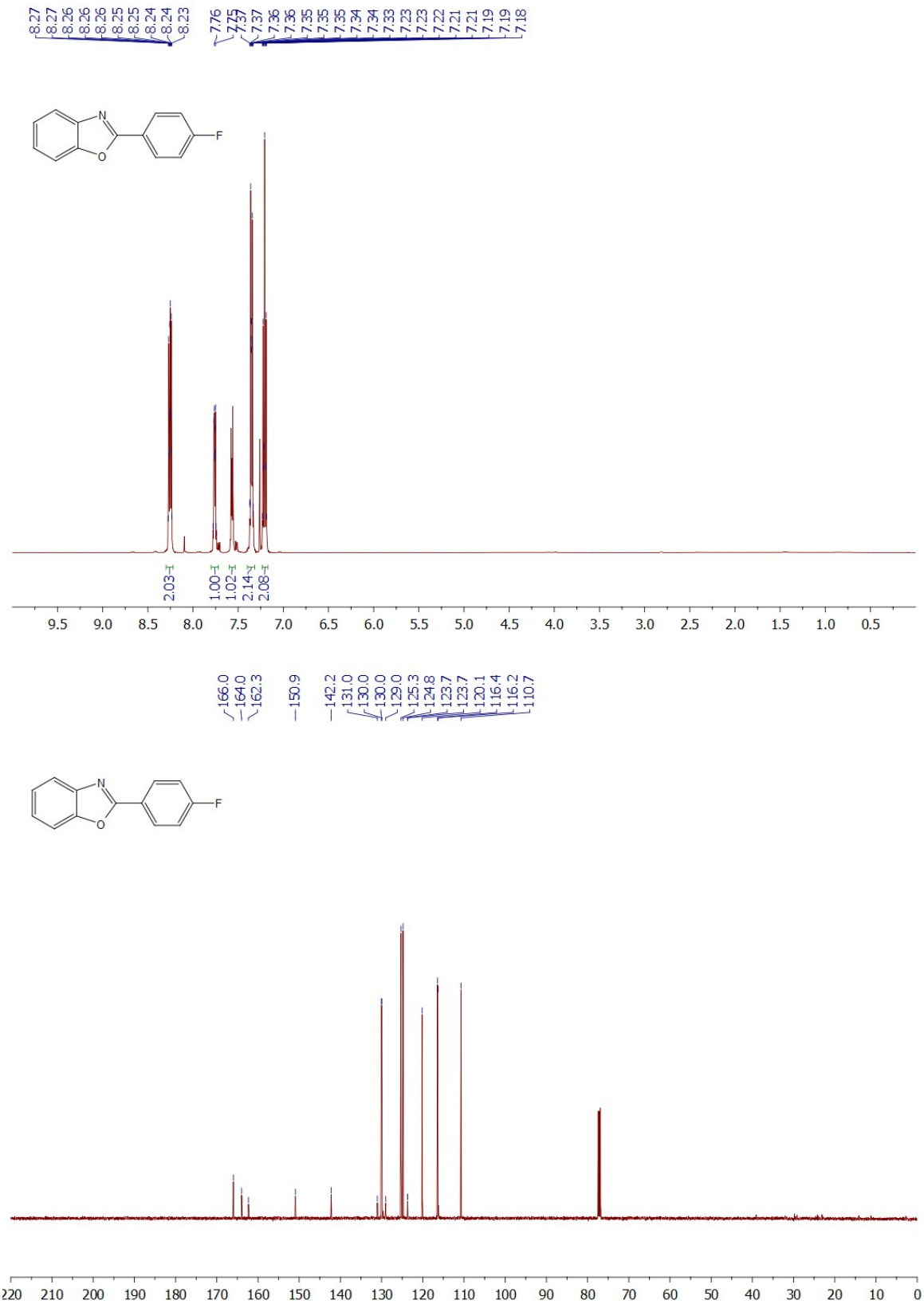

Fig. S28. ^{1}H (top) and ^{13}C (bottom) NMR spectra of 2-(4-fluorophenyl)benzoxazole.

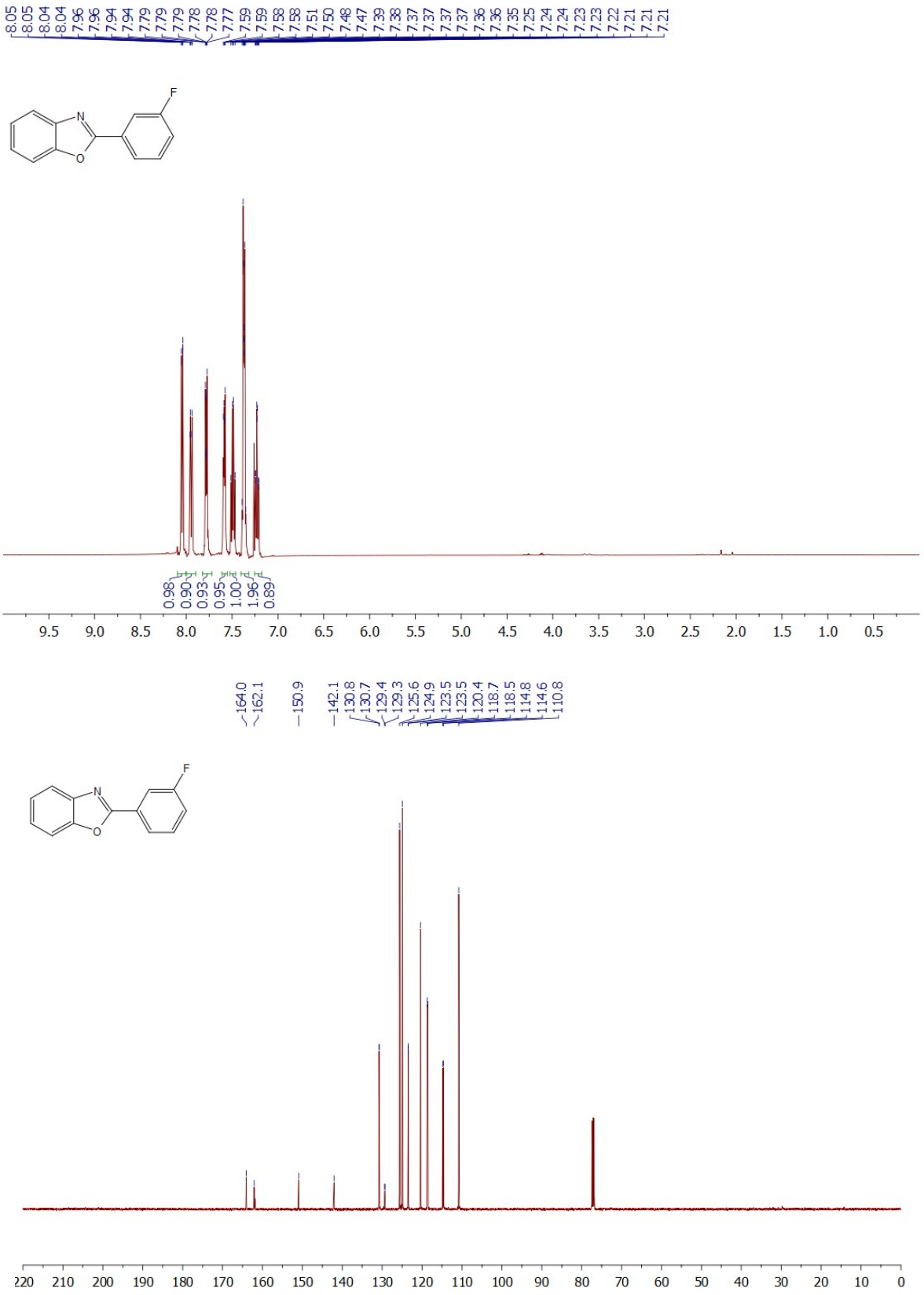

Fig. S29. ^{1}H (top) and ^{13}C (bottom) NMR spectra of 2-(3-fluorophenyl)benzoxazole.

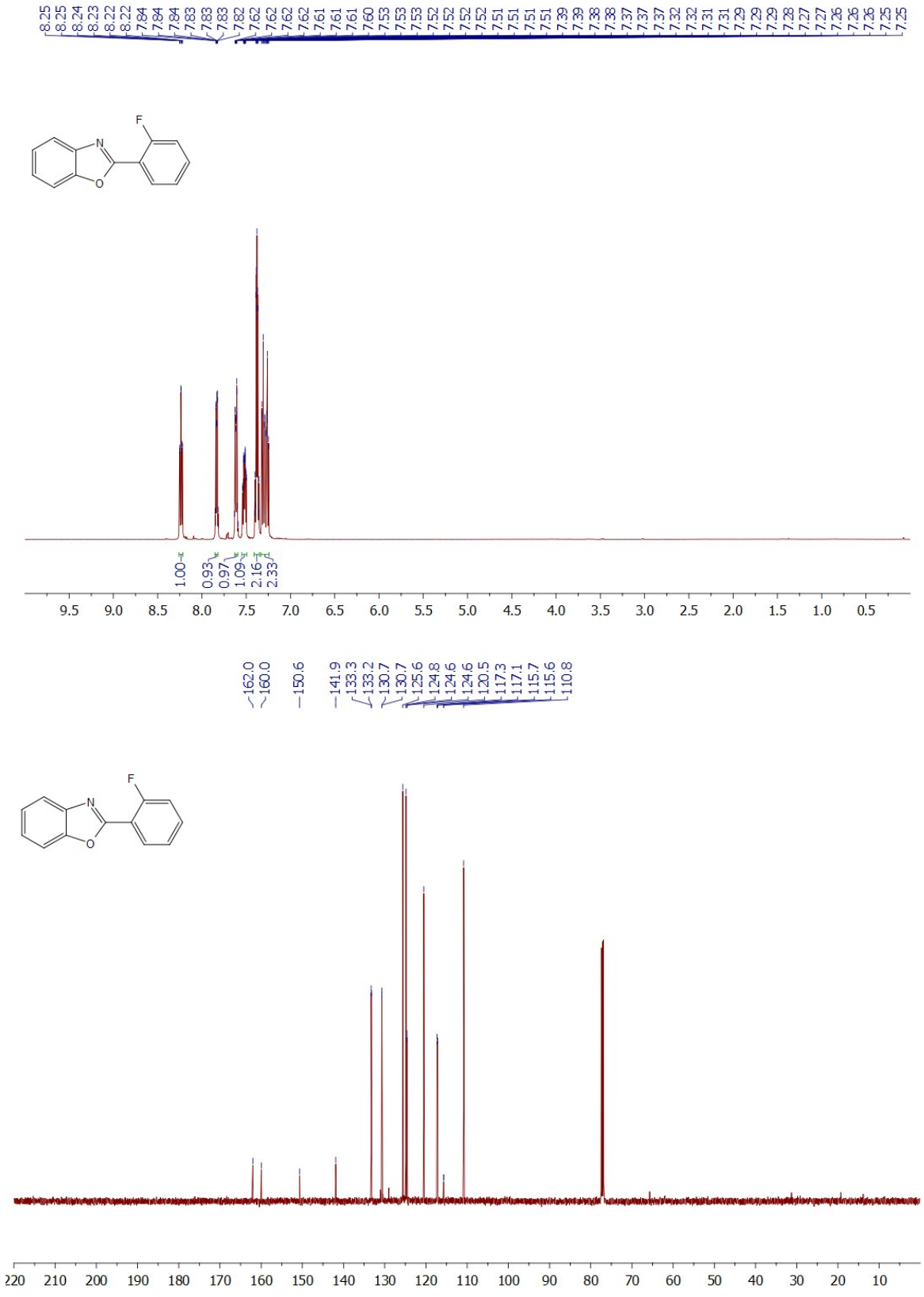

Fig. S30. ^{1}H (top) and ^{13}C (bottom) NMR spectra of 2-(2-fluorophenyl)benzoxazole.

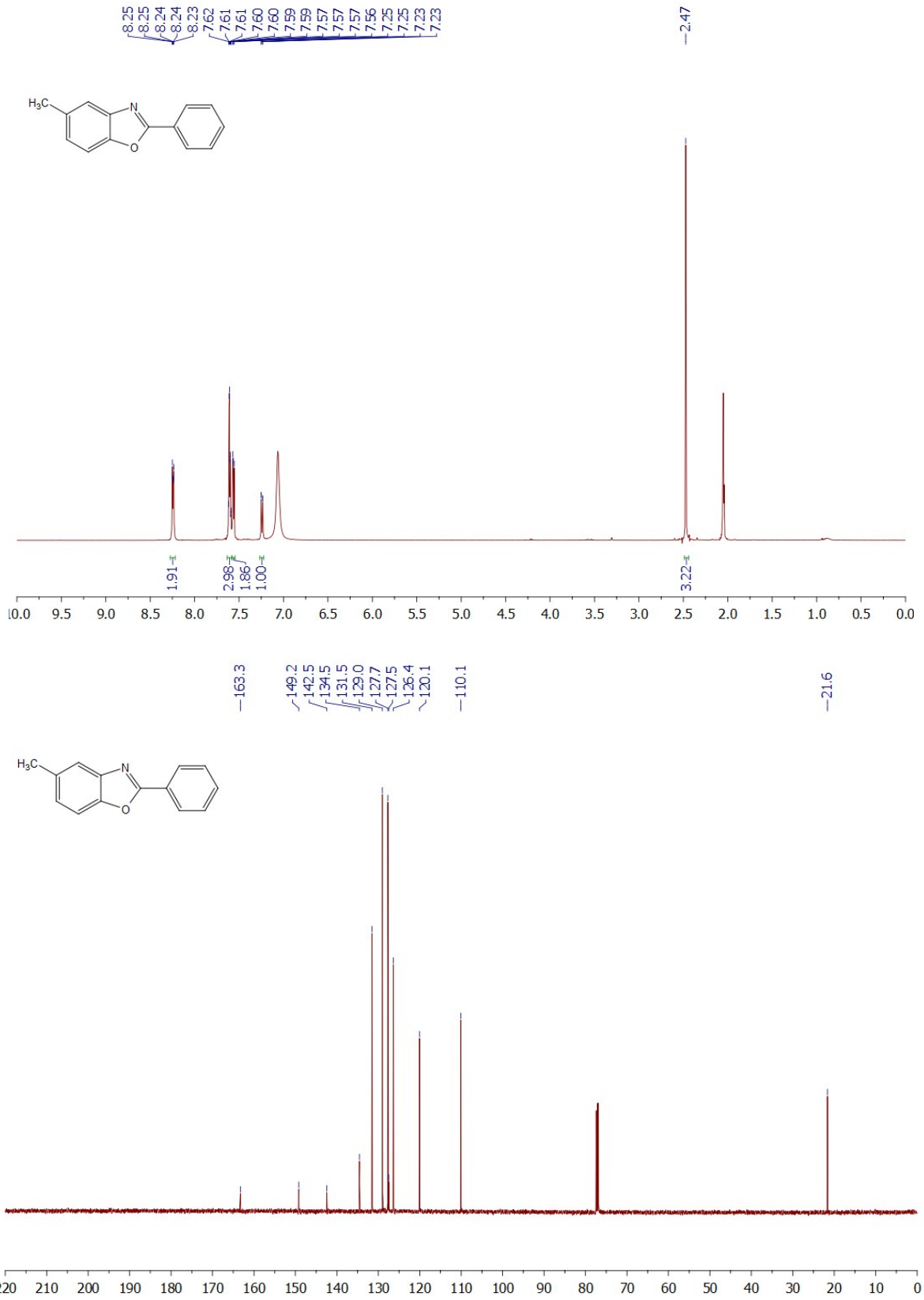

Fig. S31. ^{1}H (top) and ^{13}C (bottom) NMR spectra of 5-methyl-2-phenylbenzoxazole.

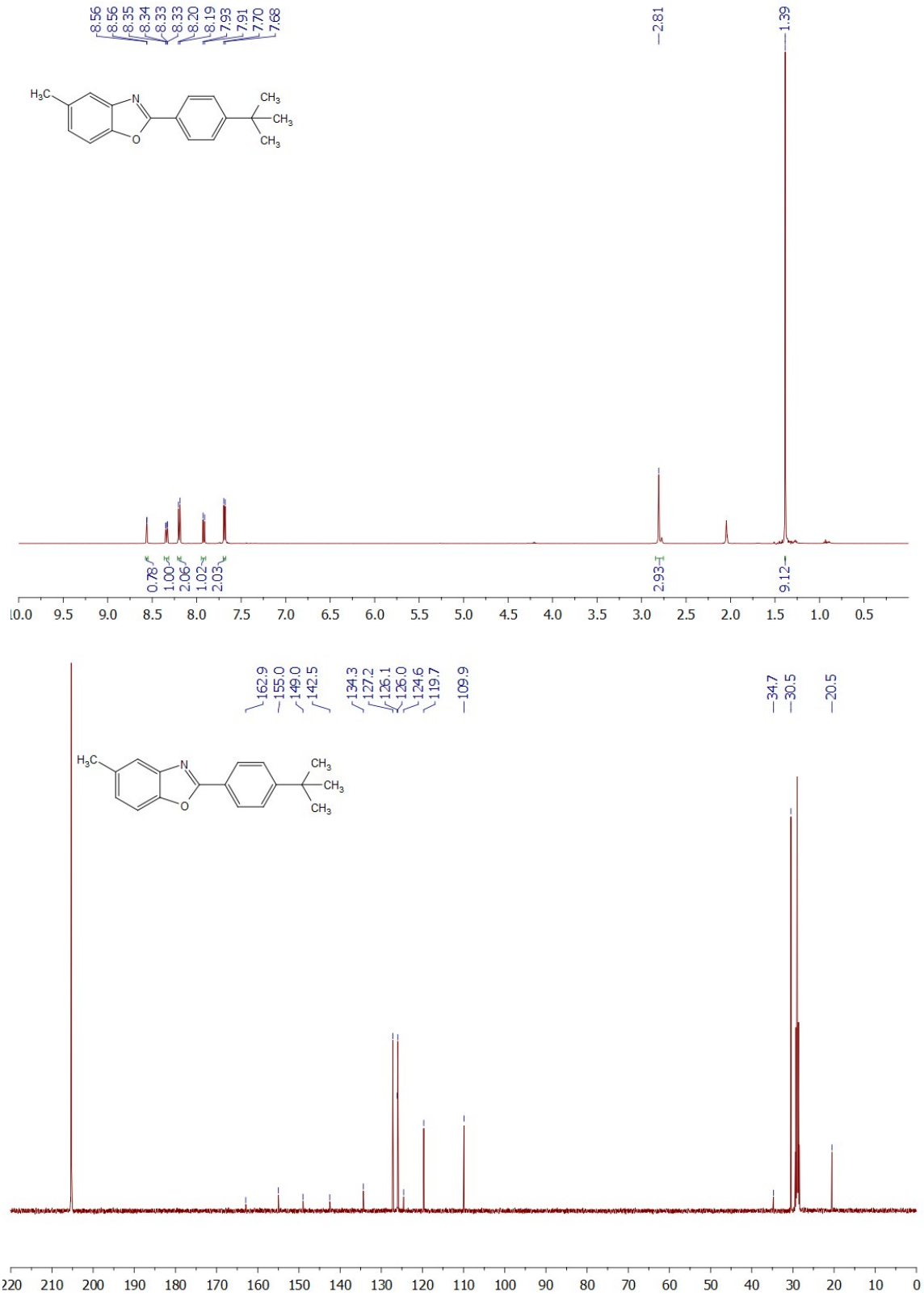

Fig. S32. ^{1}H (top) and ^{13}C (bottom) NMR spectra of 5-methyl-2-(4-*tert*-butylphenyl)benzoxazole.

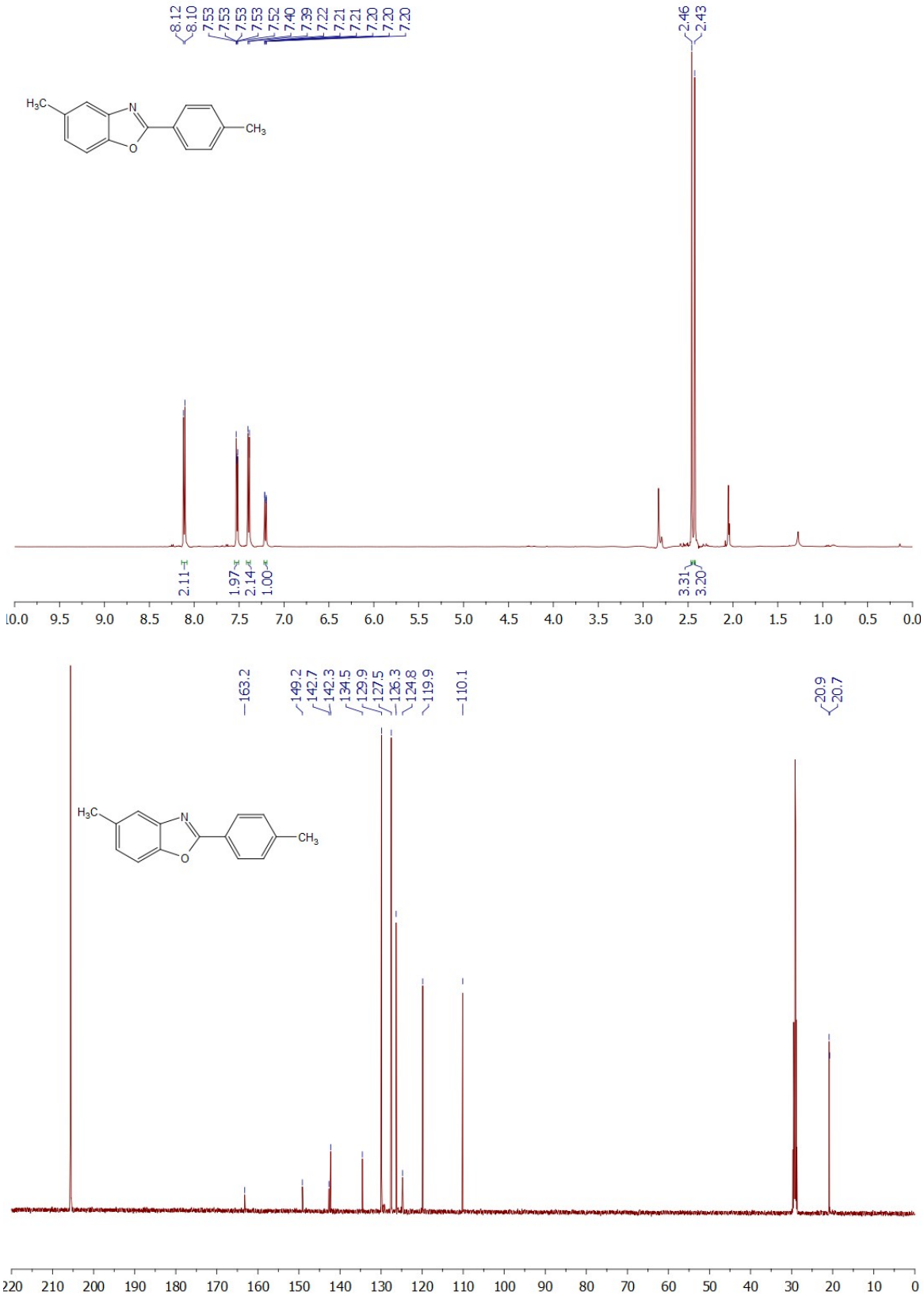

Fig. S33. ^{1}H (top) and ^{13}C (bottom) NMR spectra of 5-methyl-2-(*p*-tolyl)benzoxazole.

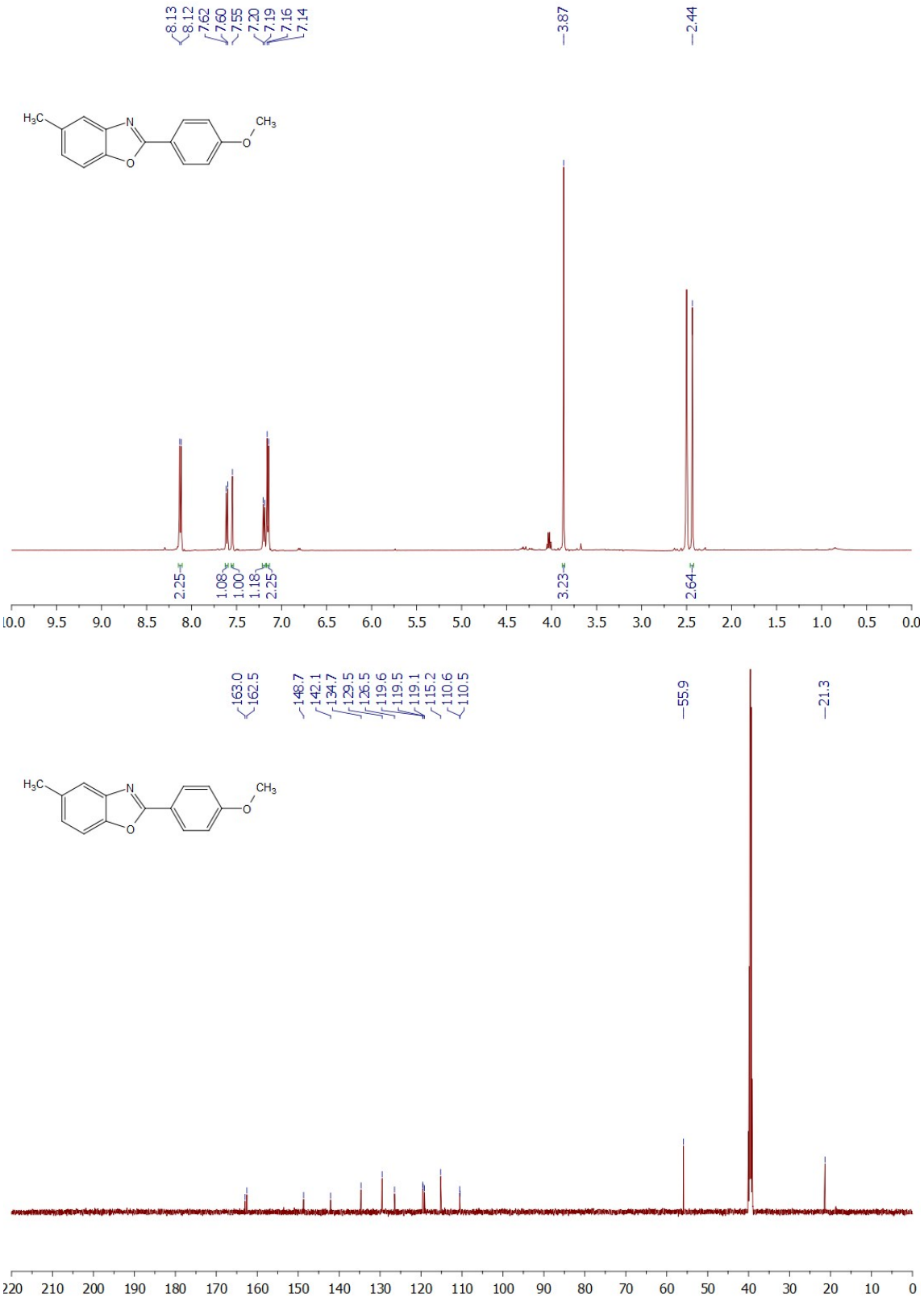

Fig. S34. ^{1}H (top) and ^{13}C (bottom) NMR spectra of 5-methyl-2-(4-methoxy-phenyl)benzoxazole.

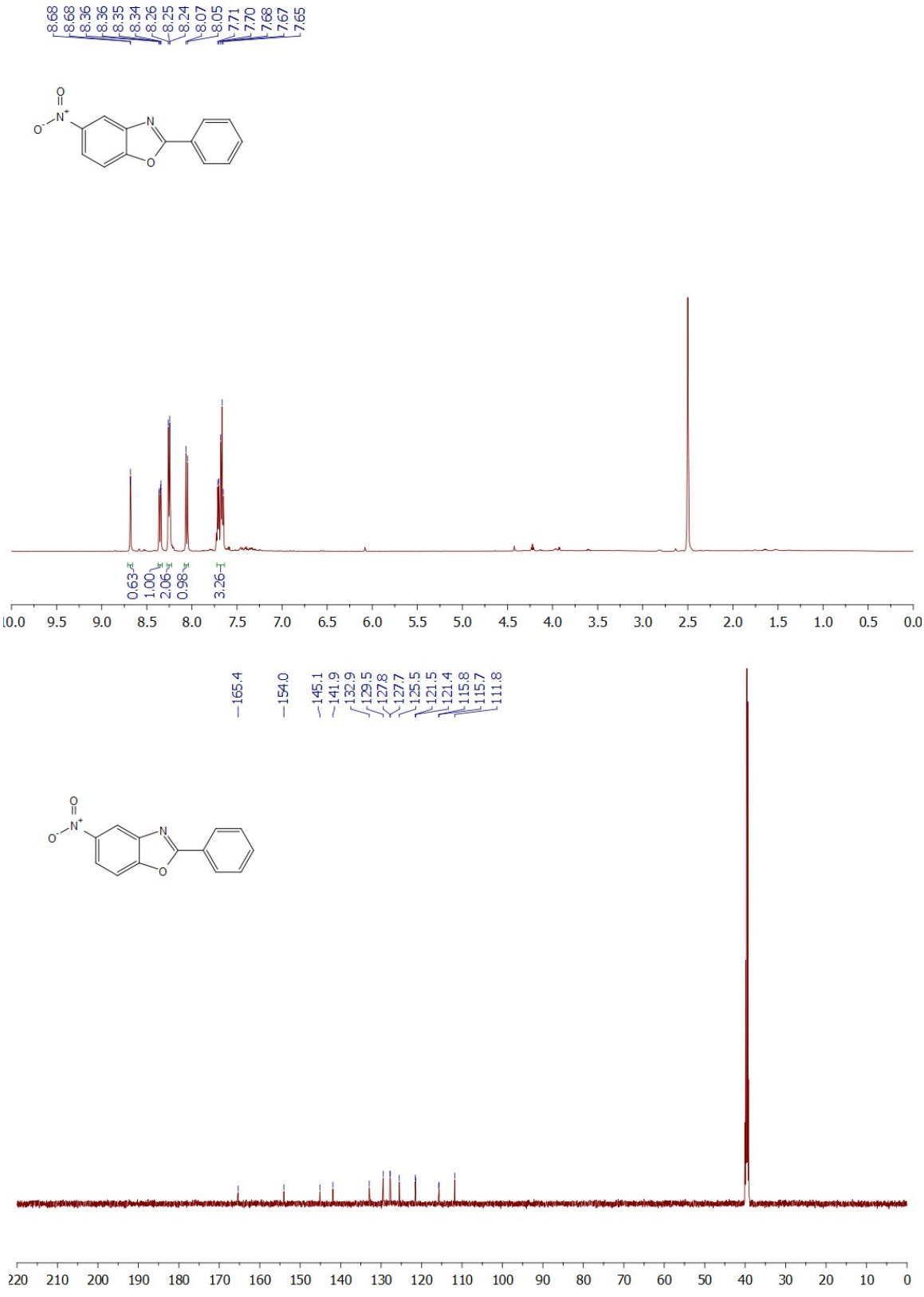

Fig. S35: ^{1}H (top) and ^{13}C (bottom) NMR spectra of 5-nitro-2-phenylbenzoxazole.

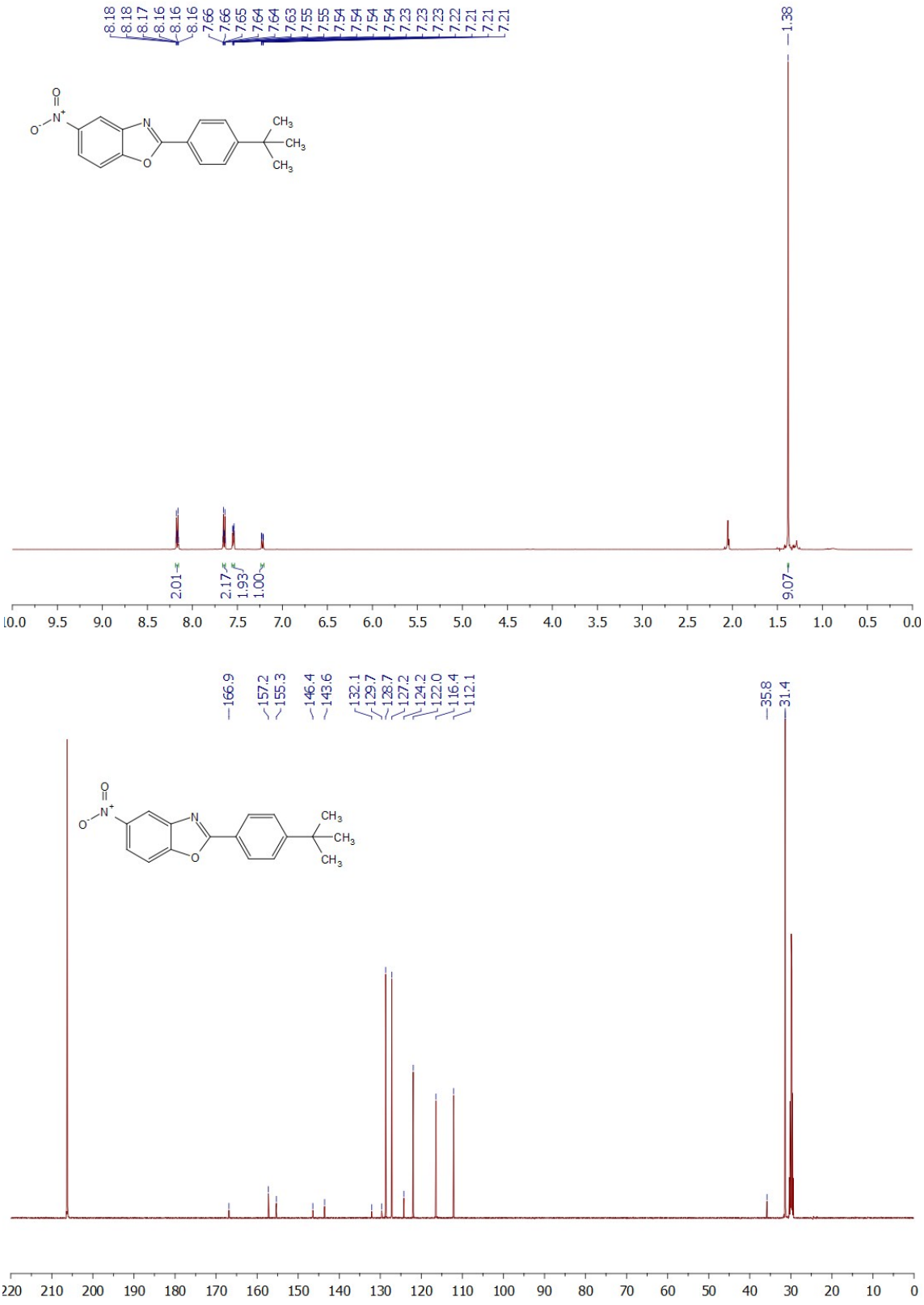

Fig. S36. ^{1}H (top) and ^{13}C (bottom) NMR spectra of 5-nitro-2-(4-*tert*-butylphenyl)benzoxazole.

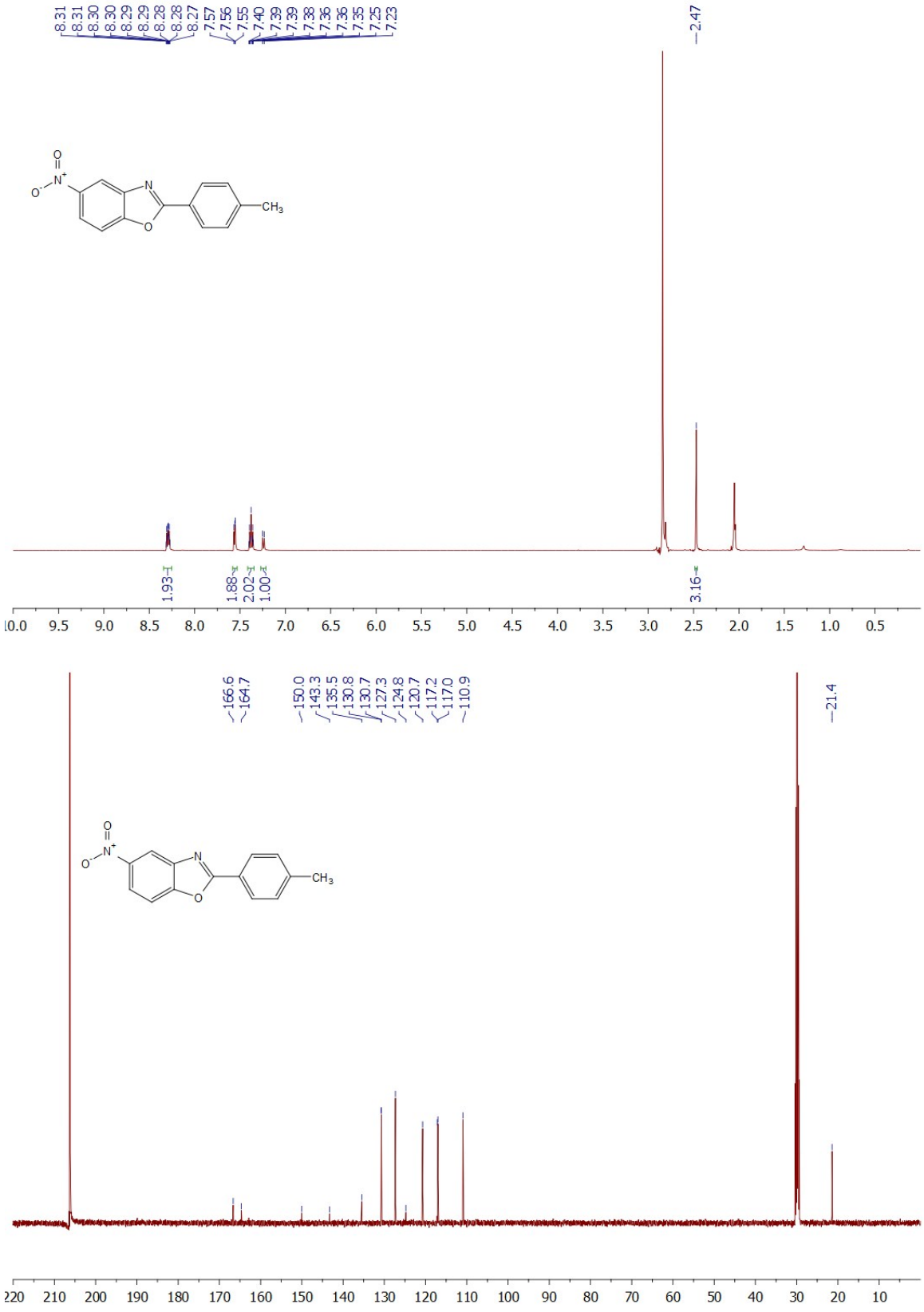

Fig. S37. ^{1}H (top) and ^{13}C (bottom) NMR spectra of 5-nitro-2-(*p*-tolyl)benzoxazole.

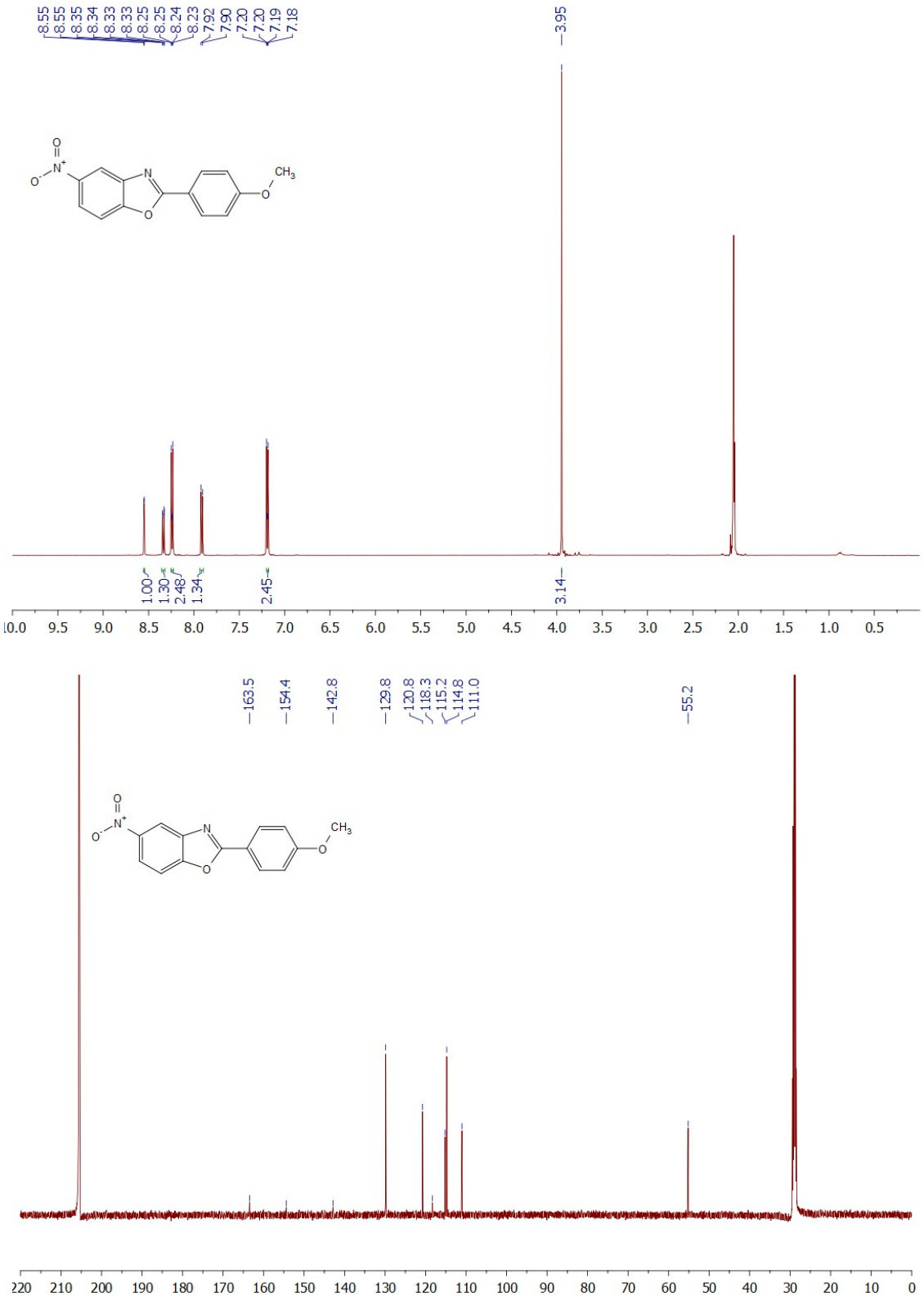

Fig. S38. ^{1}H (top) and ^{13}C (bottom) NMR spectra of . 5-nitro-2-(4-methoxyphenyl)benzoxazole.

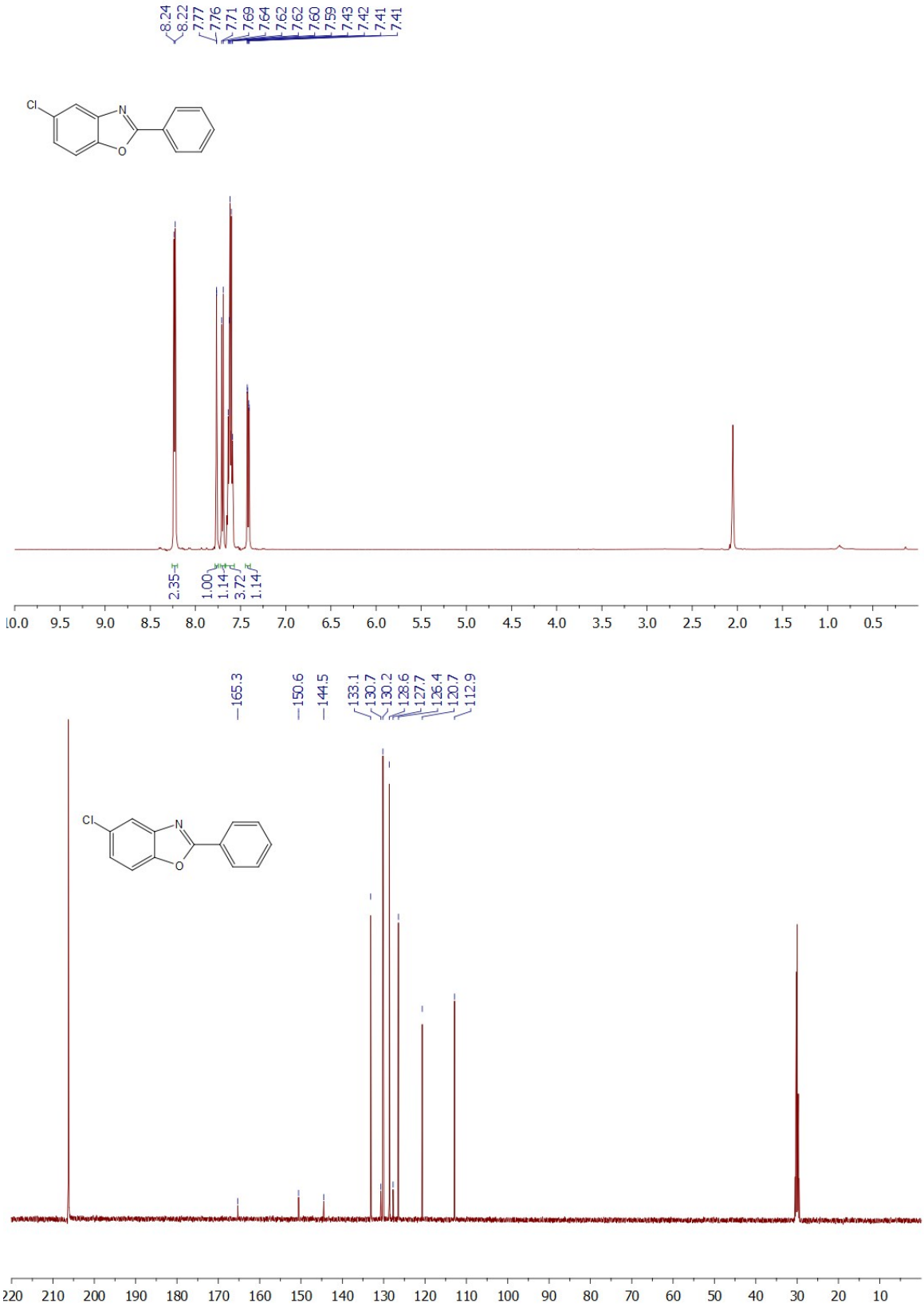

Fig. S 39. ^{1}H (top) and ^{13}C (bottom) NMR spectra of 5-chloro-2-phenylbenzoxazole.

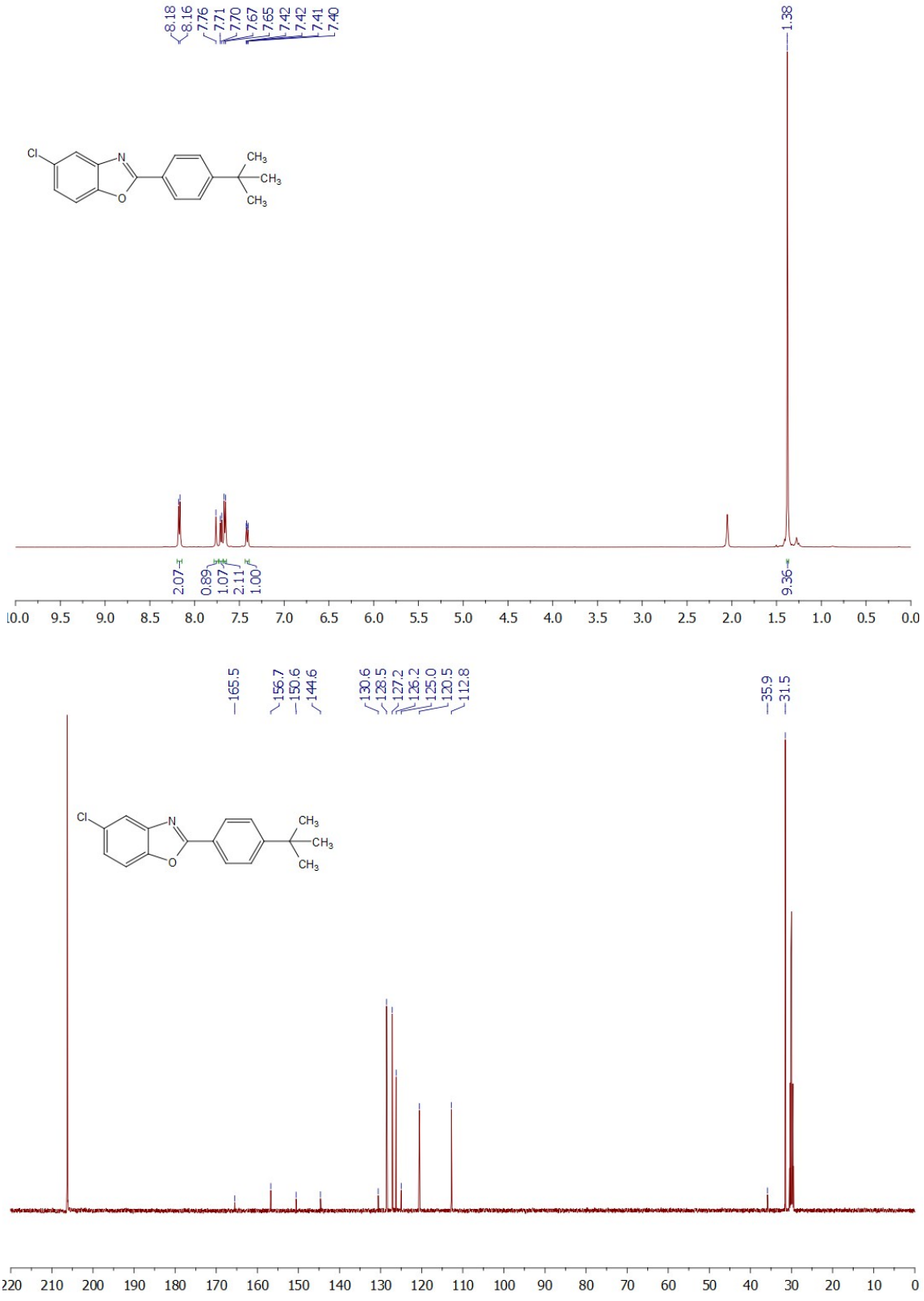

Fig. S40. ^{1}H (top) and ^{13}C (bottom) NMR spectra of 5-chloro-2-(4-*tert*-butylphenyl)benzoxazole.

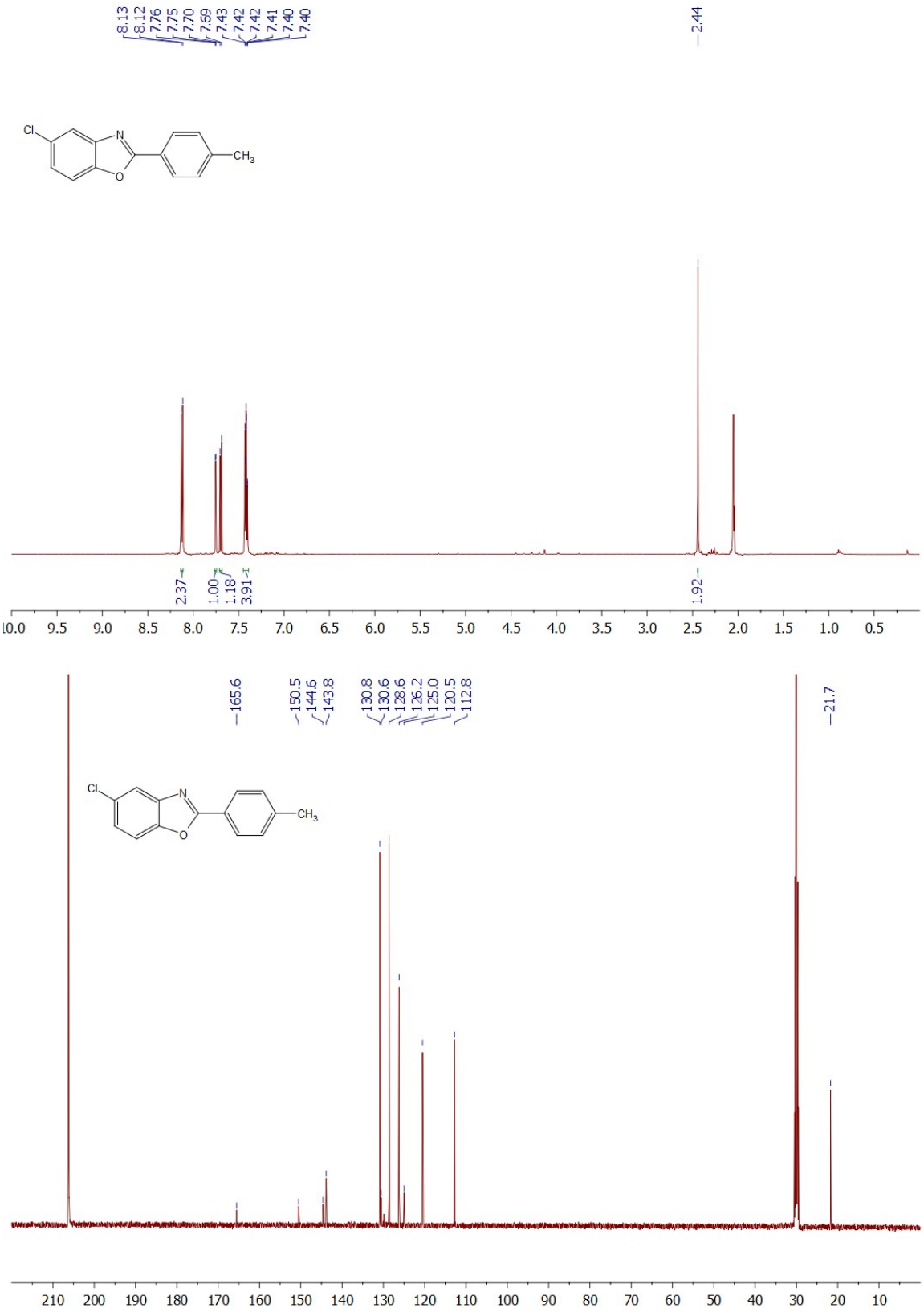

Fig. S41. ^{1}H (top) and ^{13}C (bottom) NMR spectra of 5-chloro-2-(*p*-tolyl)benzoxazole.

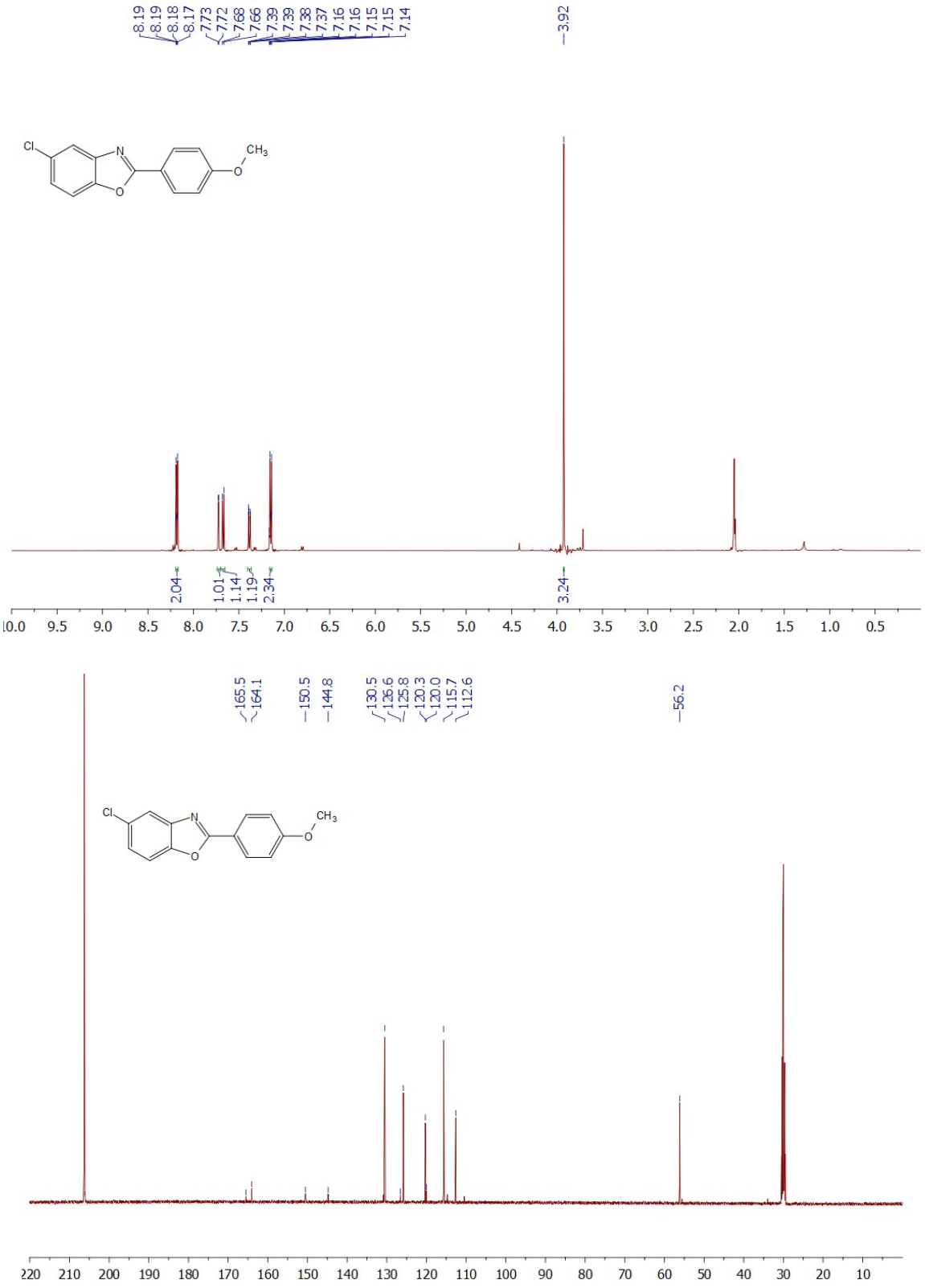

Fig. S42. ^{1}H (top) and ^{13}C (bottom) NMR spectra of 5-chloro-2-(4-methoxyphenyl)benzoxazole.

References

1. J. Jiang, F. Gándara, Y.-B. Zhang, K. Na, O. M. Yaghi, W. G. Klemperer, *J. Am. Chem. Soc.*, 2014, **136**, 12844.
2. A. Schaate, P. Roy, A. Godt, J. Lippke, F. Waltz, M. Wiebcke, P. Behrens, *Chem. Eur. J.*, 2011, **17**, 6643.
3. T. L. H. Doan, H. L. Nguyen, H. Q. Pham, N.-N. Pham-Tran, T. N. Le, K. E. Cordova, *Chem. Asian J.*, 2015, **10**, 2660.